Theses and Dissertations

5-1-2014

Monitoring Changes in Hemodynamics Following Optogenetic Stimulation

Seth Thomas Frye
University of Wisconsin-Milwaukee

MONITORING CHANGES IN HEMODYNAMICS FOLLOWING OPTOGENETIC STIMULATION

by

Seth Frye

A Thesis Submitted in

Partial Fulfillment of the

Requirements for the Degree of

Master of Science

in Engineering

at

The University of Wisconsin-Milwaukee

May 2014

ABSTRACT

MONITORING CHANGES IN HEMODYNAMICS FOLLWING OPTOGENETIC
STIMULATION

by

Seth Frye

The University of Wisconsin-Milwaukee, 2014
Under the Supervision of Professor Ramin Pashaie

The brain is composed of billions of neurons, all of which connected through a vast

network. After years of study and applications of different technologies and techniques,

there are still more questions than answers when it comes to the fundamental functions

of the brain. This project aims to provide a new tool which can be used to gain a better

understanding of the fundamental mechanisms that govern neurological processes

inside the brain. In order for neural networks to operate, blood has to be supplied

through neighboring blood vessels. As such, the increase or decrease in the blood

supply has been used as an indicator of neural activity. The neural activity and blood

supply relationship is known as neural vasculature coupling. Monitoring the

hemodynamics is used as an indicator of neurological activity, but the causal relationship

is an area of current research.

Gaining a better understanding of the coupling of neural activity and the surrounding

vasculature provides a more accurate methodology to evaluate regional neural activity.

The new optical technology applied in this project provides a set of tools to both

stimulate and monitor this coupling relationship. Optogenetics provides the capability of

stimulating neural activity using specific wavelengths of light. Essentially this tool allows

for the direct stimulation of networks of neurons by simply shining one color of light onto

the brain. Optical Coherence Tomography (OCT), another new optical technology applied in this project, can record volumetric images of blood vessels and flow using only infrared light. The combination of the two optical technologies is then capable of stimulating neural activity and monitoring the hemodynamic response inside the brain using only light.

As a result of this project we have successfully demonstrated the capability of both stimulating and imaging the brain using new optical technologies. The optical stimulation of neural activity has evoked a direct hemodynamic effect as anticipated through neural-vasculature coupling. Changes in blood velocity, flow and dilatation were all recorded using the high resolution and high speed capabilities of the OCT system.

TABLE OF CONTENTS

LIST OF FIGURES

Chapter 1: Introduction and Background

1.1 Motivation

The brain is composed of billions of neurons, all of which are connected through vast networks. After years of study and application of different technologies and techniques, there are still more questions than there are answers. Recent advances in optical technology have provided new methods of studying the brain in ways not available before. Using new optical techniques we can now stimulate the brain *in vivo* in order to study the vast interconnected neural network within using only light. The network of neurons in the brain controls and governs all neurological activity in the body either directly or indirectly. Studying these networks in order to see where these control circuits begin and end, as well as how they function has become more feasible now than ever before.

Directly monitoring neural networks is a very difficult task *in vivo*. Instead of directly monitoring the activity in networks of neurons, indicators are typically used. For example, we can monitor the neuron's energy source, the blood supply, as a primary indicator of neural activity. This indirect neural network monitoring technique is used in many current *in vivo* brain studies, fMRI, PET, NIR, etc [1]. But the coupling relationship between the neural activation and the hemodynamic response is still an active area of current studies.

The aim of this project is to use new optical technologies to stimulate neural activity while simultaneously optically imaging the vasculature in the brain. Using Optogenetics, a recently

developed optical technology, neural activity is stimulated or suppressed with specific wavelengths of light [2] [3]. The cerebral vasculature is recorded using another new optical technology, Optical Coherence Tomography (OCT), simultaneously which uses infrared light [4]. The combination of these two new technologies allows for the stimulation of neural activity at one wavelength while imaging at a different wavelength with no interference between the two optical modalities. In other words, in this project we demonstrate the possibility of developing purely optical instrumentation to stimulate the brain using visible light while imaging the hemodynamic response with infrared light simultaneously.

In addition, we also demonstrate the proof of concept in combining optogenetics with fMRI. The project's goal is to produce neural activity using the new optical technology while recording neural activity using standard *in vivo* neural monitoring techniques. Validation of this new technique will provide a new tool to precisely stimulate neural networks and monitoring the brain's processing information. In the end, the anticipated outcome is the production of to provide proof of concept neural activity must be produced using optogenetics and simultaneous recording of activity throughout the brain. This allows for the discovery of the details of the dynamics of the micro-circuits of the brain and the mechanisms of information processing.

1.2 Optical Coherence Tomography

Optical Coherence Tomography (OCT) is a new optical imaging tool that has opened many new possibilities in biological studies [5]. OCT has been used recently to image the biological structures in the brain [6]. Using only infrared light, OCT can record volumetric images of biological tissues, fluid flow and *in vivo* micro-vasculature [4] [7]. Simply scanning the surface of the brain with a laser is all that is needed to collect enough information to map out networks of blood vessels, the blood velocity and flow. For this reason, OCT technology was developed and customized in our lab to be incorporated into the neural-vasculature coupling project.

OCT is based on the Michelson - Morley interferometer where light is interfered with itself in order to precisely determine distances [5]. The main components of the system are a light source, beam splitter, reference path and sample path (Figure 1). Light from the light source is split, for example 50:50, where half travels the length of the reference path and the other half travels the length of the sample path.
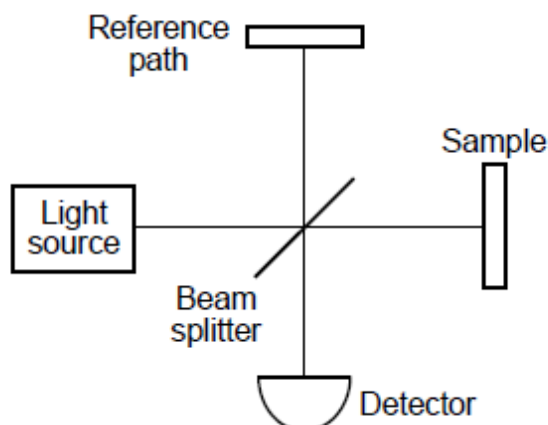
Figure 1: Michelson type Interferometer composed of low-coherent light source, beam splitter, reference path, sample path, and detector [5].

For OCT, fiber optic patch cables are used for both the reference and sample beam path to reduce the need of system alignments. When the two path lengths are at equal distances, a constructive interference pattern emerges, which is detected as an increase in amplitude. This pattern of interference is observable within the length of coherence. The interference pattern is recorded between the sample and reference path while the length of the reference path was changing, seen in Figure 2a. OCT uses a broadband, low-coherent light source, where the interference signal is detected as wave-packet [8] as seen in Figure 2b.
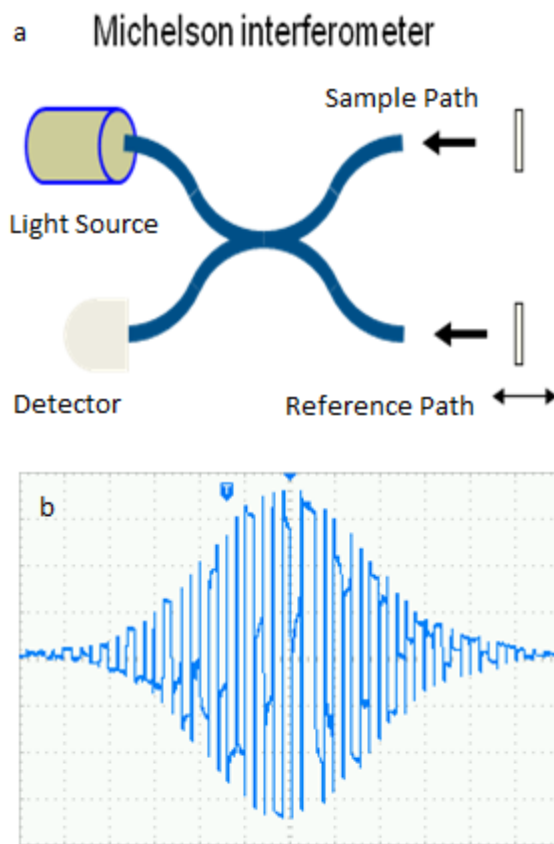
Figure 2: a) Fiber optic based Interferometer and low-coherence interference Michelson interferometer with reference path changing. b) Interference signal recorded at detector as reference path changed.

Initially, when we were scanning a sample with the OCT the length of the reference path was changed using a high precision micro positioning system. A single axial scan (A-scan) was performed by changing the length of the reference path and recording the interference amplitude at each position. A single A-scan contains multiple interference patterns that vary in amplitude based on loss, reflection and transmission of the surrounding tissue. A sample A-scan can be seen in Figure 3 where the raw interference signal has been rectified and demodulated to demonstrate the amplitude of interference relative to position of the mirror in the reference path.
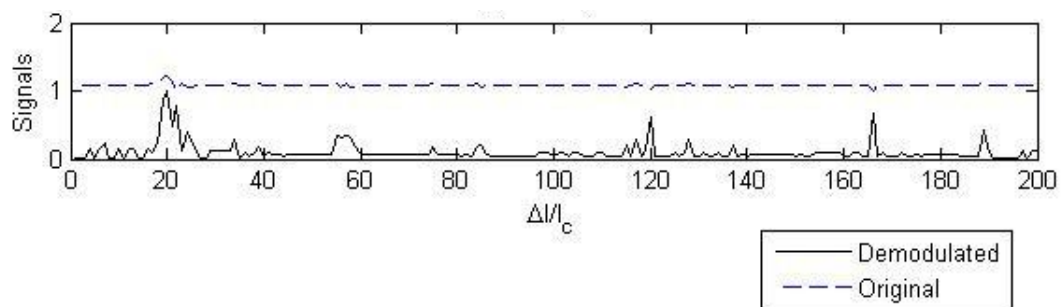
Figure 3: Axial scan (A-scan) demonstrating interference signals at different positions along the A-scan.

In order to produce the desired cross sectional image, sequential A-scans must be captured across the sample. A sequential line of A-scans across a sample (B-scan) are collected and processed. The result of this process is a two-dimensional cross section of the image, as shown in Figure 4. The image is grayscale with intensities based on the amplitude of the interference signal at that position.
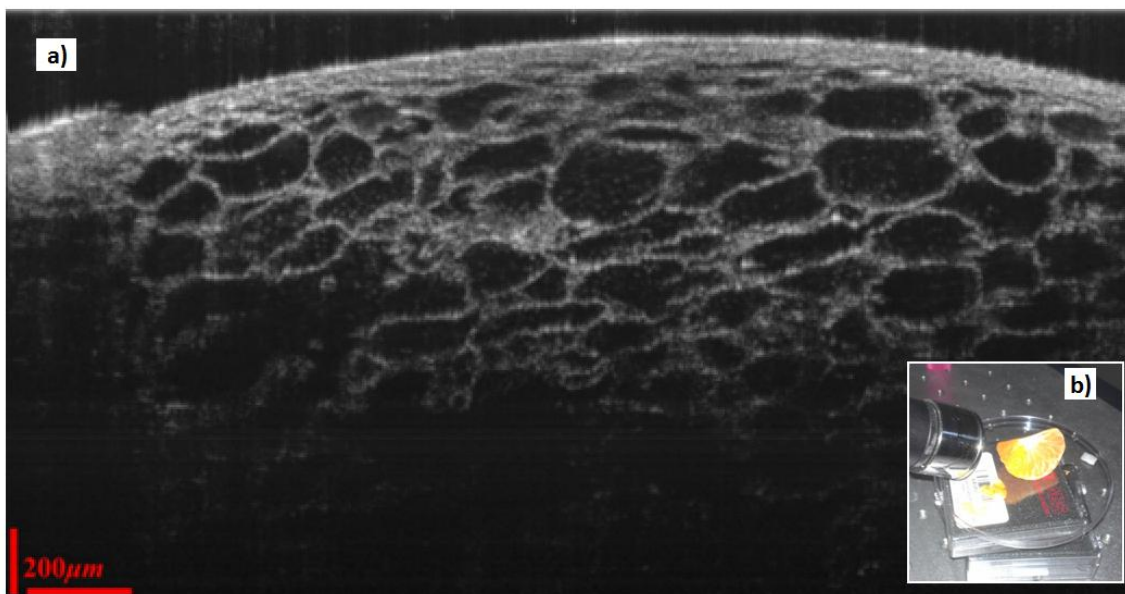
Figure 4: a) Cross section image of orange scanned with OCT. b) Image of OCT system scanning orange.

To produce three-dimensional images, the B-scans are also acquired sequentially over the surface of the sample. A raster scanning pattern is used where the X coordinate is captured in each B-scan and the Y coordinates are scanned over sequential B-scans. The final volumetric data set then contains the interference signal at each precise three-dimensional coordinate. Three-dimensional sets of data can be represented as cross sectional slices which are projected onto a plane for visualization, as shown in Figure 5.
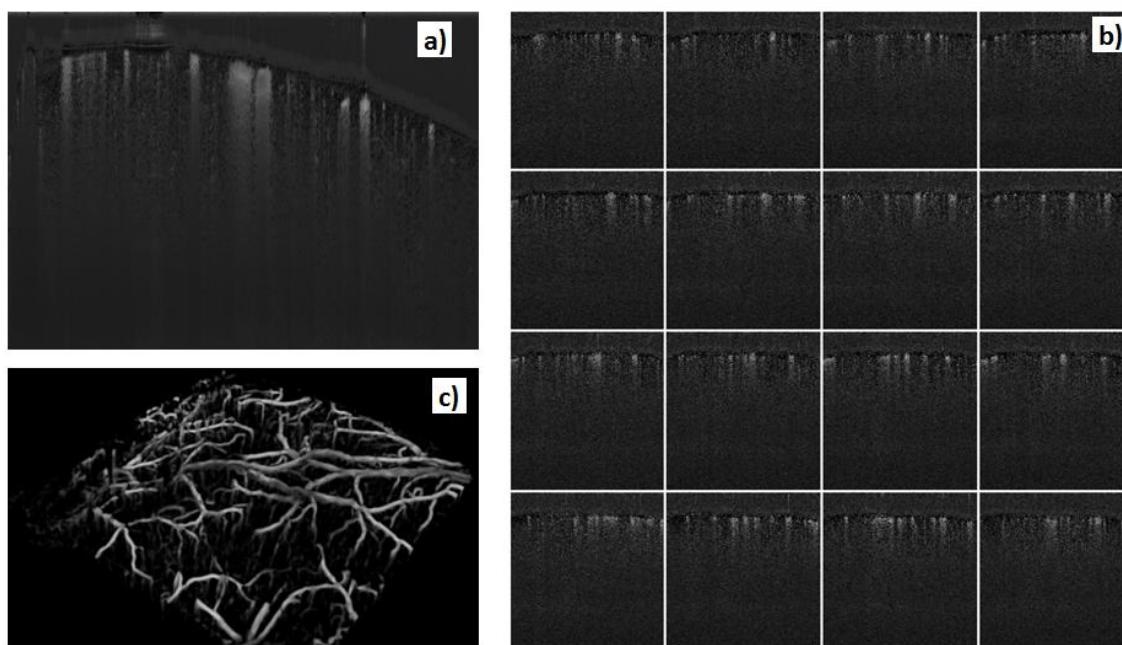
Figure 5: a) Single cross sectional image of sample is recorded. b) Multiple cross sectional images are recorded sequentially across the sample. c) The images are then stacked in order to create a three-dimensional image.

All of the OCT scanning techniques up to this point, known as Time Domain imaging, have relied on mechanically manipulating one of the paths in the interferometer. This introduces two limitations when translating this technology for *in vivo* experiments. The first is a source of error in position which is dependent on the accuracy and repeatability when changing path lengths.

Another major limit is the long scanning time required to change the path length for each A-scan. To overcome these challenges, a new OCT scanning technique was implemented to improve all key concerns with accuracy, repeatability and the scanning time.
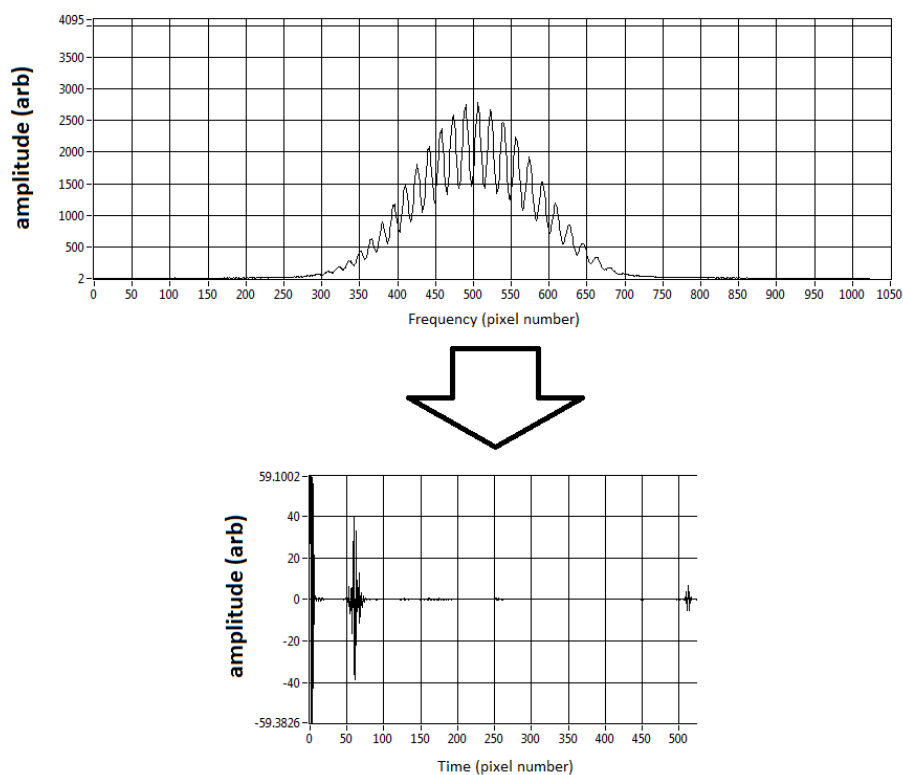
Figure 6: Spectral (Frequency) Domain is transformed into time domain using Fourier transform [9].

Spectral Domain OCT (SD-OCT) imaging, also known as Fourier Domain (FD-OCT), does not require the manipulation of the reference path. Instead it uses the spectrum of the light source to find interference along an A-scan. In other words, the spectral data collected is transformed to find the position of interference along a single A-scan. Figure 6 demonstrates the process in which spectral data captured over a range of different frequencies are transformed and represented in a format similar to the time domain data. This capability removes the previous

concerns over the accuracy and repeatability since there are no more moving components. Plus, most importantly, the scanning time will improve drastically since the entire A-scan will be recorded in one spectral domain acquisition.

High speed and improved accuracy come with a small cost when switching to the spectral domain [10]. That small cost is that the spectral domain requires more signal processing in order to reconstruct each A-scan similar to what was produced before in the time domain. The data processing and transforms performed on the spectral domain require higher performance software rather than the precise hardware positioners previously used. The new data processing components of the spectral domain imaging may have a cost in processing power, but also provides more options when analyzing the data.

In addition to the high accuracy and high speed capabilities, the spectral domain also allows monitoring of changes in the phase and frequency of the sample. For example, by recording the changes in phase in the SD-OCT data, we can identify moving particles, such as fluid flow. On top of capturing fluid flow, changes in frequency also indicate the velocity of the moving particle. For these reasons, the SD-OCT system is the ideal device for measuring blood velocity and flow *in vivo* and was selected for our project.

1.3 Optogenetics

The project presented here has aimed to provide a new set of optical tools which aim to help improve the capabilities of neuroscience field. New optical technologies available now have the capacity to both stimulate and suppress neural activity using only light. Optogenetics useslight sensitive proteins that are used to stimulate neural activity when exposed to specific wavelengths of light [11]. Optogenetics allows us to manipulate neural activity by exposing the brain tissue to appropriate wavelengths of visible light [12] [13]. In our experiments we stimulated the brain by only using blue light (473nm laser) and were able to monitor the induced hemodynamic activity with the SD-OCT imaging system.

Neural stimulation centers on the physiology of the neuron itself. The neuron is made up of a cell body (soma), cellular extensions (dendrites) and nerve signal transport pathways (axons). Biological neurons are networked together using synapses, see Figure 7. In the resting state, a neuron maintains an electric potential across the cellular membrane. When the cell membrane of the neuron is depolarized, for example as a result of external stimulation, the neuron becomes active by generating action potentials, which are sharp changes in the membrane potential of the cell. Activity then transfers from neuron to neuron within a specific neural network via synaptic couplings. Arrays of such neural networks develop the architecture of the brain and provide mechanisms for data processing.
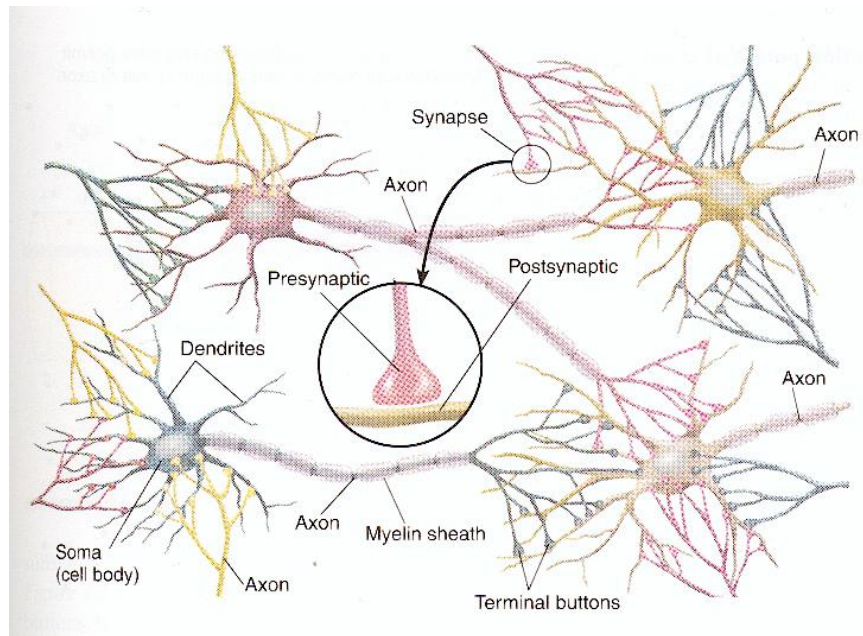
Figure 7: Networks of biological neurons, with labeled components [14]

Until recently, neural stimulation was controlled and monitored at the cellular level mostly using electrodes. Electric probes are inserted into or near neurons where a current is applied to depolarize, or stimulate, a single neuron or a local network of neurons. Also, an electrode can be inserted to monitor a single neuron or a network of local neurons. While the process may be very straight forward, it has two major limitations, first of which is the limited accuracy of stimulation. In a very simple picture we can assume that an electric field radiates outward in a uniform sphere and any neuron or network within that sphere can be stimulated with no specificity. Using this mechanism, all cell types in the region are stimulated. A direct consequence of this stimulation mechanism is generation of multiple side-effects since some cell types that we do not intend to target are stimulated. Electric stimulation and monitoring provide data for many of the essential functions of the brain, but are now limited in precision and accuracy in comparison to new technologies.

Optogenetics, a new optical technology, provides both high accuracy and precision along with

the high speed and targeting capabilities that are achieved using molecular genetics techniques.

Optogenetics is based on the combination of light sensitive proteins derived from light sensitive

bacteria (Chlamydomonas reinhardtii) and new genetic modification technologies [11]. The

genetic code of the optically sensitive protein is added to the genetic material of a specific

neuron to make the neuron sensitive to light [15]. Exposure to one color, or wavelength, of light

activates the genetically modified cell, see Figure 8. Since the stimulation is based on light it is

now possible to target individual or large networks of neurons simply by exposing them to

appropriate wavelengths. By using new optical technologies, high accuracy and precision will

provide more advanced capabilities.
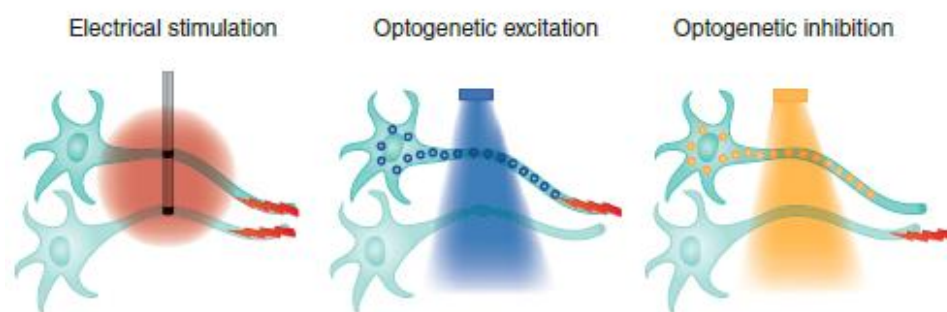
Figure 8: Diagram comparing electric neural stimulation, Optogenetic stimulation and Optogenetic inhibition [11]

1.4 Functional Magnetic Resonance Imaging

A common technology used to study the brain is Functional Magnetic Resonance Imaging (fMRI). Initially MR imaging provided very high resolution anatomical images of the body's soft tissues, including the brain. MRI technology is based on using very large powerful electro-magnets and short radio pulses. Simply using the body's tissues electromagnetic properties the MRI can recorded changes in radio waves that result in very high resolution 3D images. In the 1990s scientists found that by measuring the properties of the blood in the brain, MRI technology could also be used to image brain activity [16]. This non-invasive approach is based on the relationship between neural activity and blood flow. Nonetheless, the main indicator of neural activity in fMRI recording, the Blood Oxygenation Level Dependent (BOLD) signal is still not completely understood. The optical technology developed in this project potentially provides new information about neural-hemodynamic coupling and will help researchers to better understand the source of the BOLD signal.
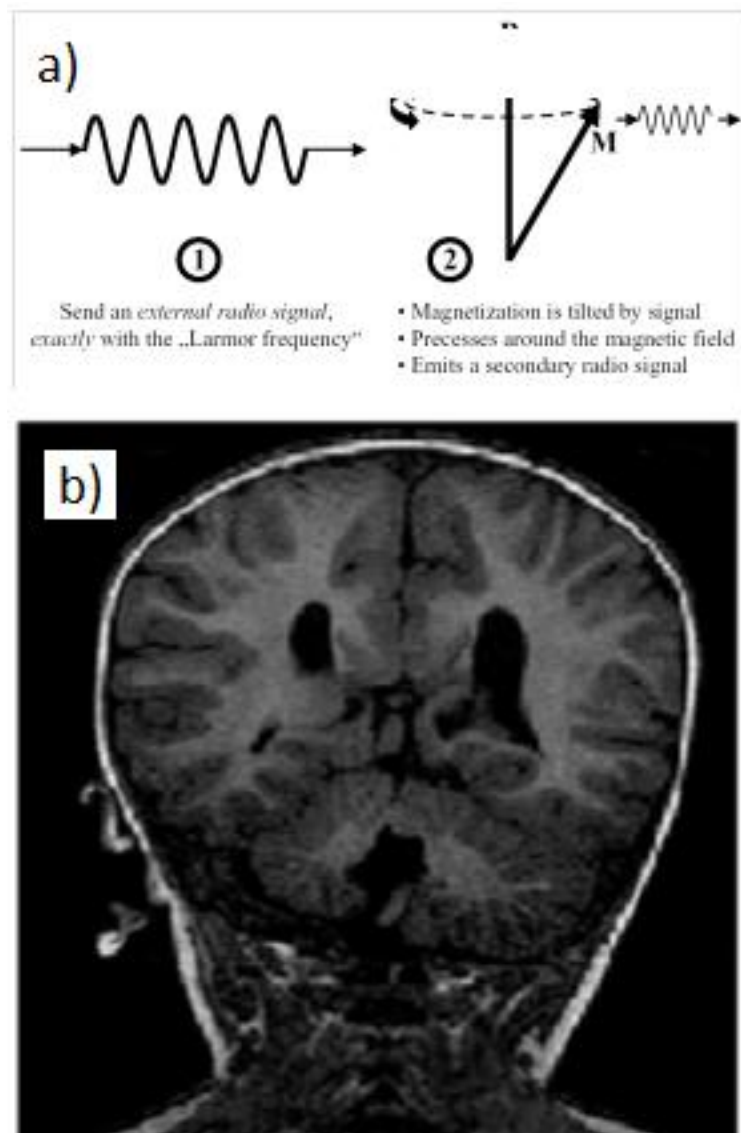
Figure 9: a) RF and MR interaction to produce secondary signal. b) Typical MR anatomic image [16].

Imaging using MR technology is based on electromagnetic fields and how they interact with tissue. Every molecule in the body is made up of atoms that contain both protons and electrons. Generally speaking, the proton and electron interaction contains a 'spin' that results in a very small electromagnetic field that is completely random in the body. When a very large powerful magnet is applied, 10,000 times stronger than the earth's magnetic field, the spins are aligned

with the field. Electromagnetic waves are applied, such as radio waves, to interact with the

aligned spins. A simple diagram of this process is presented in Figure 9a. After the radio waves

interact with the spins, the time it takes to return to the initial state, the relaxation time, is

recorded. The relaxation time is then used to determine the anatomic structure of the tissue, in

other words, produce an anatomic image similar to the typical image shown in Figure 9b.
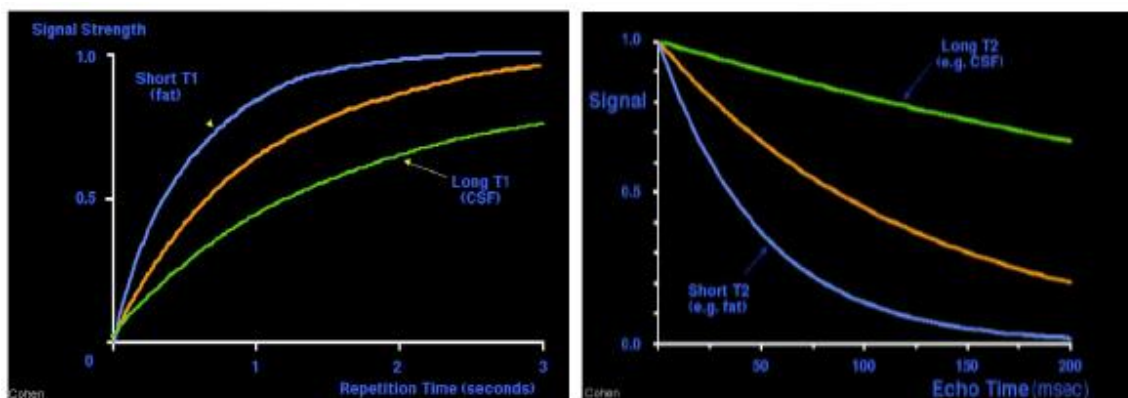
Figure 10: T1 and T2 relaxation times for fat and cerebral spinal fluid (CSF) in the brain [16]

Two scanning techniques were used, T1 and T2 to image different tissue in the body [16]. The

T1 graph in Figure 10 measures how quickly the spin realigns with the magnetic field. While the

T2 graph measures how quickly the spin releases radio waves as it relaxes back to a point of

equilibrium. Another technique, known as T2*, looks for the inhomogeneous effects of the T2

signal on the magnetic field. By monitoring T2* the MR scanner can detect changes in the

relaxation time for a specific molecule. Since blood oxygenation levels change the spin

orientation of the molecule, the change in relaxation time is recorded with a T2* scan [17].

Using the basis that neurological activity requires more oxygenated blood and produces more

deoxygenated blood than the surrounding area, the Blood Oxygenation Level Dependent (BOLD)

signal can then be used as an indirect indicator of neurological activity. Functional MR imaging

(fMRI) uses the BOLD signal as a standard technique to monitor neurological activity across a

wide field of view in the brain.

While fMRI technology is noninvasive and can monitor the BOLD signal in the brain, it also has

some tradeoffs. Ignoring the major resources that fMRI technology requires, it also has inherent

limitations in temporal and spatial resolution. High definition scans at the sub millimeter level

are now possible with very powerful magnetic coils, which are used in this project. But in order

to achieve a high resolution scan, multiple scans must be taken and averaged over a long period

of time. For wide field anatomical scans this technique is often used, but for sub millimeter

resolution motion artifacts become more and more problematic. Also, the scanning time to

record the BOLD signal is over hundreds of seconds and again must be repeated multiple times

to average the signal. Since we are interested in the neural vasculature coupling as optical

stimulation is applied, multiple stimulation and recording sequences will be used in order to

average the wide field BOLD signal. Adding new optical technology, e.g. Optogenetics, to the

fMRI will help improve the capabilities of both technologies and provide a new tool to study the

functions of the brain.

1.5 Neural-vasculature coupling

To study and understand how the brain processes data, we must gain a better understanding of its fundamental functions. The focus of this work will be on the relationship between neural activity and how it couples with hemodynamic functions. Neurological processes and neural network activity require a blood supply from surrounding blood vessels as an energy and oxygen source. An increase or decrease in neural activity is followed by an increase or decrease in blood flow to the active area. This coupling between the neural networks and the surrounding vasculature provides an indirect method to monitor neural activity. Monitoring hemodynamics is a common indicator used to study neural activity, but the causal relationship is still an area of active research. New optical technology applied in this project provides a new set of tools to both stimulate and monitor this coupling relationship.
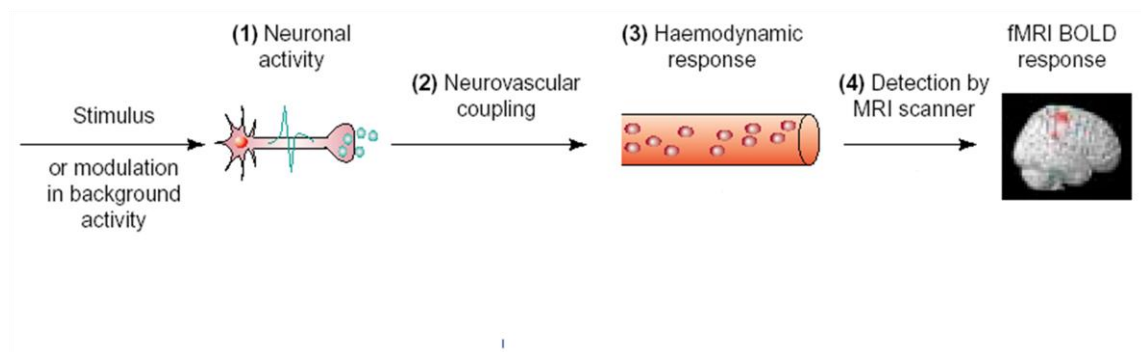
Figure 11: Neural vasculature coupling diagram connecting neural activity to the fMRI BOLD signal [18]

When neural activity is stimulated a feedback mechanism triggers the surrounding blood vessels to deliver the energy and oxygen required by the active neuron (Figure 12a). This fundamental mechanism in the brain is important in regulating neural activity but is still not completely understood. What is understood is that neural-vascular coupling triggers the dilation of blood

vessels, increases blood flow and results in the BOLD signal (Reference). It has also been observed that the increase in neural activity results in an increase in the BOLD signal [18]. It is known that local neural networks, not single neurons, are responsible for generation of the BOLD signal [19]. In addition, when the neural-vasculature mechanism is activated a forward control is sent to the source of the blood vessel in order increase the blood supply [20]. Since the local blood capillary networks do not contain any smooth muscle, the feedback must be sent upstream to the arterioles in Figure 12, larger blood vessels with smooth muscle. The arterioles dilate as a result, increasing the blood velocity and flow back downstream to the stimulated neuron's neighboring capillary network [21] [22].

The glia cells, sometimes referred to as the forgotten brain cells, are originally thought to be the 'glue' cells that make up half of the brain and simply hold other brain cells together. Only recently has it been found that glia cells perform many fundamental functions in the brain [22]. The particular cell to focus on with respect to neural vasculature coupling would be the Astroglia, which are convenient neighbors of the neurons and blood vessels. Originally thought to be 'non-essential' for neurological activity, it is now known that Glial cells interact directly with neurons and blood vessels, such as in the diagram in Figure 12. Astroglia cells are specifically responsible for monitoring synaptic activity, regulating metabolic demands and most importantly increasing blood flow [23] [24]. Studying neural vasculature coupling is more important now than before because of the role it plays in supporting and regulating neural activity in the brain.
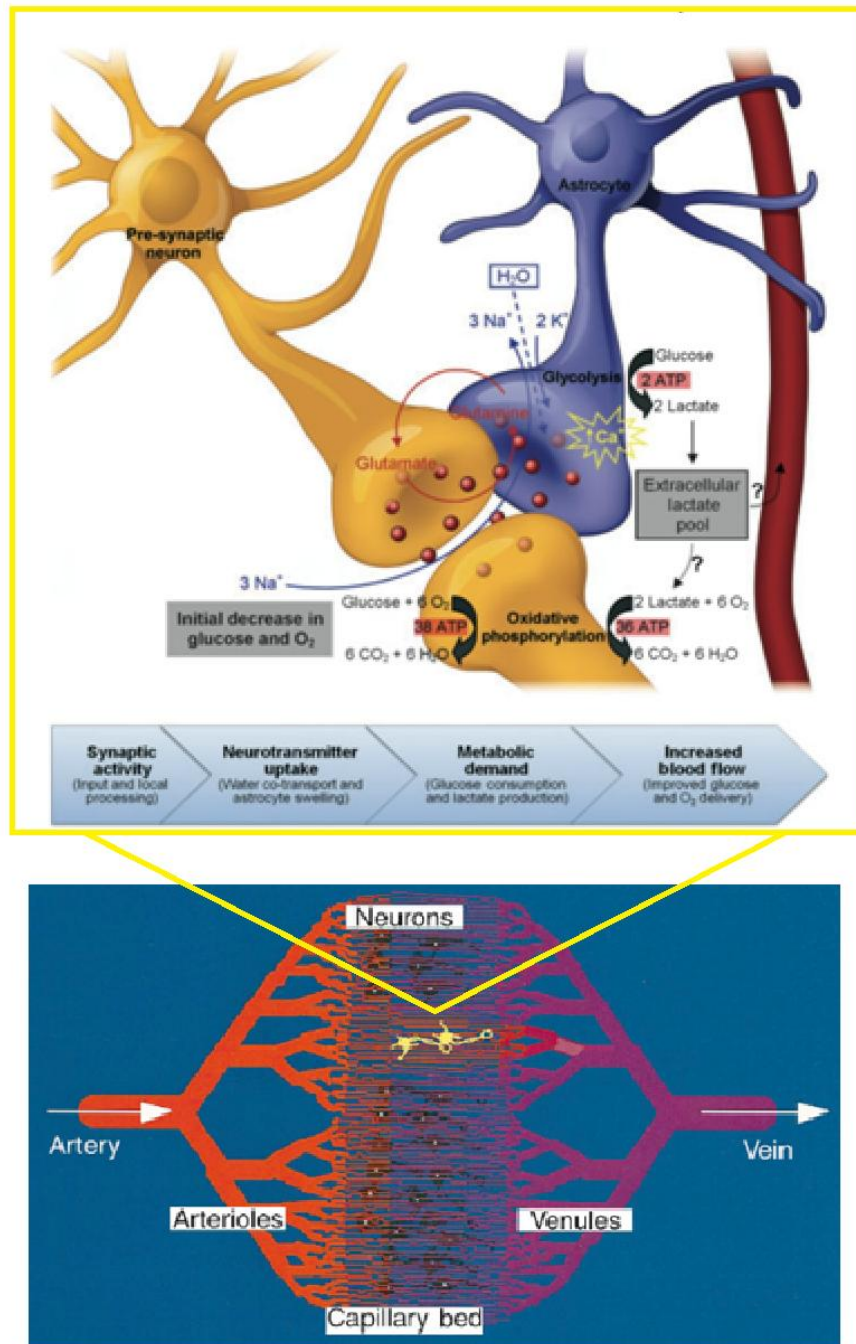
Figure 12: Diagram of vasculature starting at artery and arterioles delivering blood to the capillary bed. Changes in blood flow relative to neural activity are indicated in the venules which then deliver blood to the vein [24]. The sub-diagram highlights the functions neural-hemodynamic coupling functions of the astroglia cells [21].

Recently it was understood that the relationship between neurons and their surround vasculature network is more complex than a simple feedback mechanism [24]. In addition to the increase in blood supply, the local neural network can also route the needed oxygenated blood to a specific site. Capillary networks do not have the smooth muscle needed to constrict or dilate, instead a 'valve system' has been observed (Figure 13) that can open and close individual capillaries [23].This recent evidence suggest the precise control of the capillaries surrounding the neural networks.
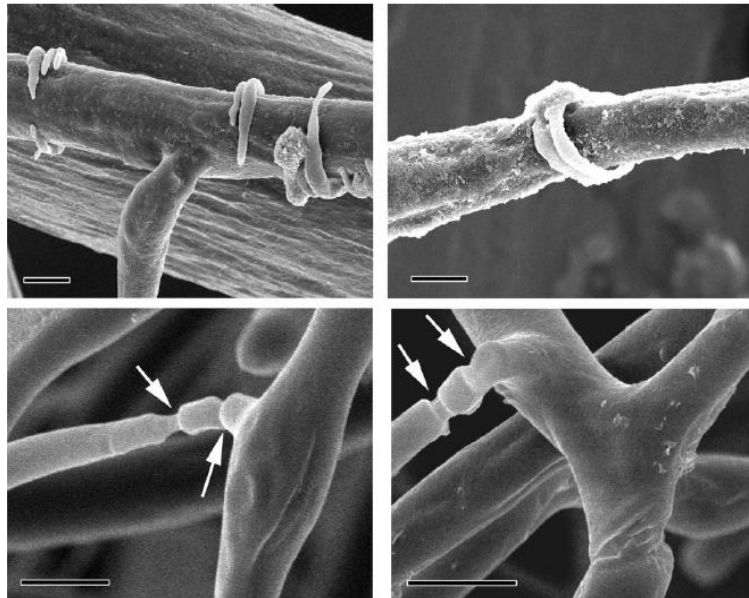
Figure 13: Scanning electron microscope (SEM) images of blood flow control structures near branch points in capillary bed demonstrate the strong coupling between precise blood flow control and neural activity. [25]

Studying neural vasculature coupling is more important now than before because of the role it plays in supporting and regulating neural activity in the brain. For this reason, the development of new tools is important to studying the effects of the relationship between neural networks and blood flow.

1.6 Summary

In order to investigate the relationship between neural and hemodynamic coupling the projects presented here will develop optical techniques to both stimulate and monitor the brain. The goals are to use Optogenetics to directly stimulate neurons in the cortex and then record the resulting changes in blood flow. Based on what has recently been reported on neural-vascular coupling [22], the resulting hemodynamic response will be observable at the arteriole level. The Optogenetic OCT project can then stimulate neural activity and monitoring the hemodynamic response at the surface of the brain. Second, the Optogenetic fMRI project can stimulate neural activity inside the cortex where the hemodynamic response will be monitored via the BOLD signal. Both new optical technologies will stimulate neural activity and measure the resulting hemodynamic response as a result of the coupling between the neural and vasculature systems.

Chapter 2: Development of Optogenetic neural stimulation and Optical Coherence Tomography cerebral vasculature imaging

This chapter will focus on the development of a system capable of stimulating and imaging the brain using recently developed optical techniques. To achieve this goal, the project should have to meet the following goals. First we should design and build the OCT optical hardware and develop the necessary software to run the OCT and process the collected data. Then, we need to plan an experimental approach to stimulate the brain with optogenetics and record the hemodynamics.

In order to image the changes in the vasculature system surrounding the neural networks, a high speed, high resolution OCT system had to be developed. Optical Coherence Tomography (OCT), a recently developed optical technology, has been used to image the cortical layers of the brain in vivo. More importantly, in 2010, it was reported [4] that OCT can monitor the change in dilation of blood vessels in the brain *in vivo* (Figure 14). The SD-OCT system developed to produce such results used a 1300nm low-coherent source with an extended broadband spectrum of 200nm. Using only broadband infrared light, OCT can image blood vessels and blood flow inside biological tissue without any dyes or any other labeling techniques. The decision was made to develop a similar system at the lab to include the Optogenetic stimulation capability as well. By simply scanning the surface of the brain with an incoherent light source OCT is able to record three dimensional images of the blood vessels and the flow of blood down inside the brain around stimulated neural networks.
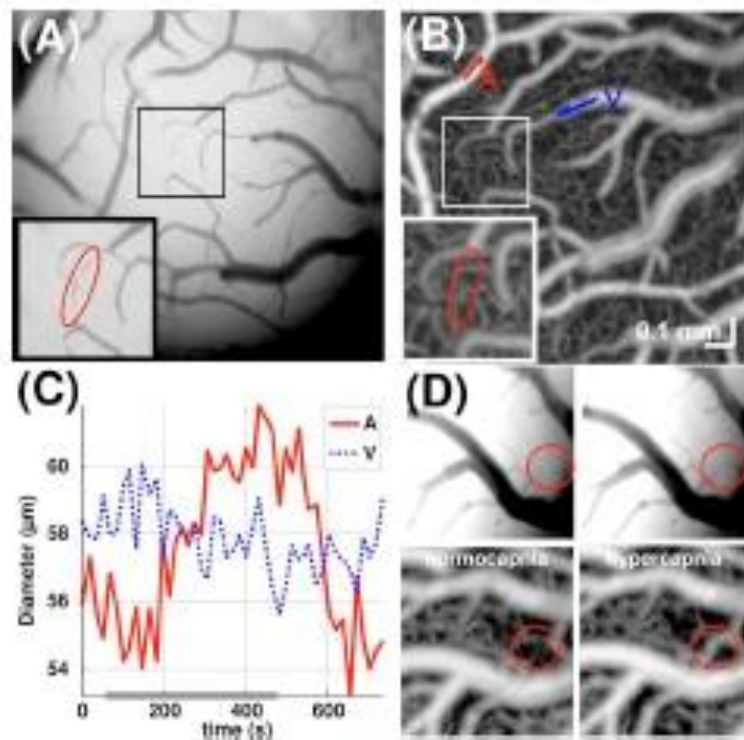
Figure 14: OCT images taken of arterials and capillaries [4]

In order to optically stimulate the neural networks inside the brain the new optically based neural stimulation technique, Optogenetics, was included. The goal of the project is to both stimulate and monitor neural-vasculature coupling using only non-invasive optical techniques. Therefore in order to simultaneously stimulate and monitor neural activity plus the hemodynamics of the surrounding blood vessels, Optogenetics was combined with OCT [26]. Since there is no Optogenetic-OCT system available when this project began a customized system had to be designed and developed in the lab.

2.1 Hardware Development

Time Domain Optical Coherence Tomography

At the very beginning of this project, an OCT system was assembled using only a few simple

parts. Since the fundamental component of an OCT is an interferometer, a fiber based

Michelson interferometer was initially constructed. The initial interferometer was built using a

fiber optic coupler (acting as a beam splitter), fiber optic patch cables, beam collimators and a

pair of mirrors. The first light source was a fiber coupled Super Luminescent Diode (SLD) with a

central wavelength of 1300nm and a bandwidth of 80nm (Covega, Inc). Figure 15 is an image of

the sample and reference paths coupled into a fiber optic interferometer, where both paths are

connected to a lens tube system, each with a gold mirror at the end. The tube system uses

micro-positioners to adjust the path lengths. A low coherent source was sent into the fiber

optic coupler and the resulting interference pattern was detected on a balanced photo detector

(Thorlabs: INT-MSI-1300, Inc). The interference signal was then observed when moving the

sample arm to the same distance as the reference arm, also known as Zero Path Difference

(ZPD). Since the light source is a low coherent laser, the interference pattern is made up of two

components. First is the central or carrier wavelength; the second being an envelope based on

the length of coherence that is determined by the bandwidth of the SLD, seen in Figure 2.
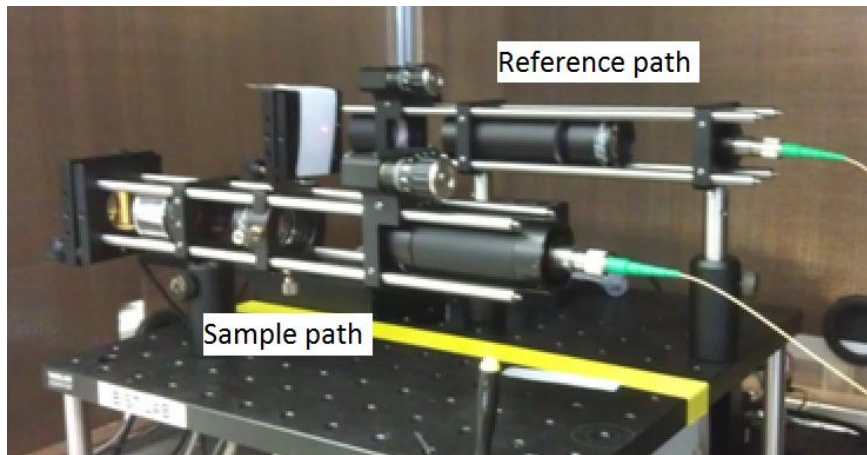
Figure 15: Image of sample and reference paths of fiber based interferometer.

After the first interferometer system was built, two scanning mirrors and an objective lens were incorporated to magnify and image a sample with high resolution. The scanning mirrors, or Galvanometers (Galvos) are two high speed, high precision electric micro-motors made up of a fast action and slow action mirror (Cambridge, inc) [27]. The fast action mirror is used for high speed scans along the X axis, while the slow action mirror is for moving along the Y-axis. The first version of the OCT scanner combined the Galvo with a telecentric 'Scan' lens so that a sample could be scanned in two dimensions (Thorlabs: LSM 03). At the beginning, the scanner, made up of the Scan lens and Galvos, was added to the sample arm in Figure 16. To record the interference pattern of the sample, the scanner performed a line scan over the sample, capturing the interference signal. The reference path was moved each time the scanner captured another line over the sample. To create a cross sectional image, sequential line scans were stacked in order to create a 2D image. Adjacent 2D images were than captured and combined in order to create a 3D image.
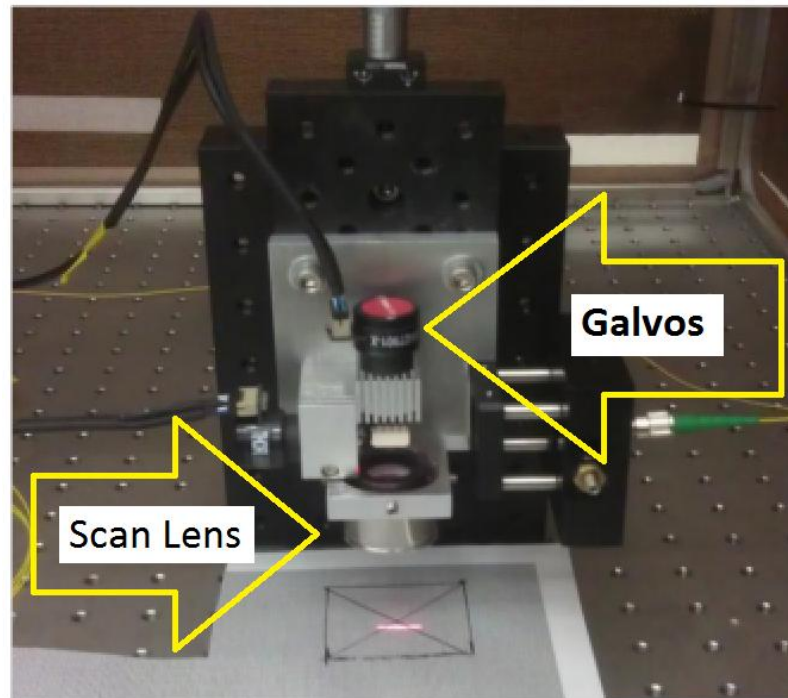
Figure 16: Image of first version of scanner performing a line scan (red line) with mounted scan lens and galvos (yellow arrows).

Since the first scanner was a basic mounting plate, it had to be upgraded so that the Galvos were enclosed and the scan lens was mounted to a lens system. A relay lens system had to be added to the scanner because the back focal distance of the scan lens was shorter than the distance to the Galvos, seen in Figure 17a. To mount and align the lens system, a lens tube had to be connected to the Galvo enclosure. The second version of the scanner was first modeled in a CAD environment (Figure 17b) and then machined on a CNC mill. The new enclosure and mounting system was also made to fit on a microscope double arm boom stand, as displayed in Figure 17c. After the new scanner was constructed, it was added to the OCT system and immediately used to scan samples.
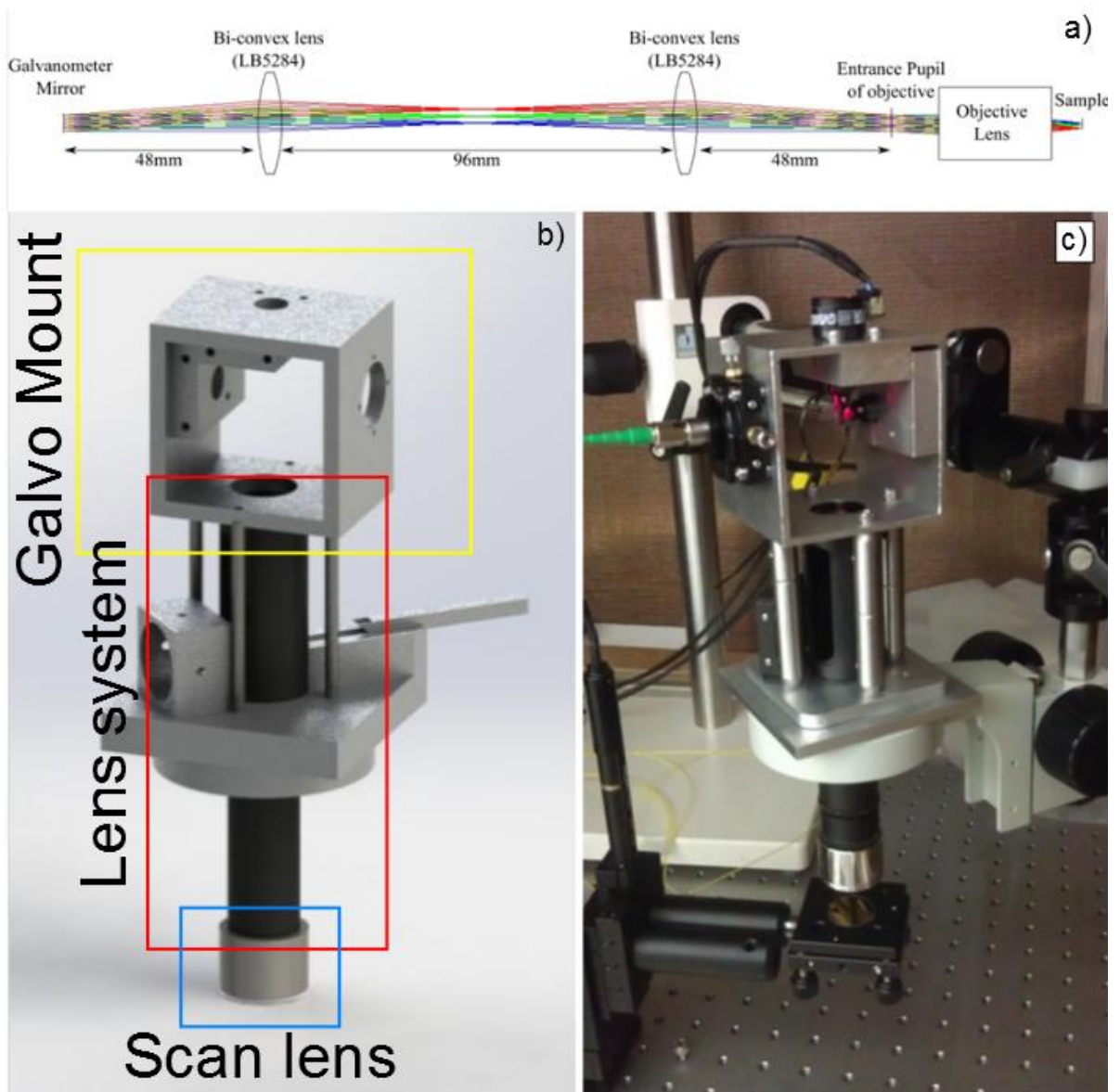
Figure 17: a) Lens relay system designed to increase back focal distance of scan lens. b) CAD model of lens system (black tube) inside custom mount. c) Fabricated mounting system with lens system, galvos and scan lens.

The first OCT system is typically referred to as a Time Domain OCT system, where the reference

path acts as a time delay mechanism. By moving the reference path the time delay is adjusted

and interference signals are collected relative to the path length. This system is capable of

producing high resolution images, but sufferers from the error due to the reference path's

mechanical positioner. More essential, the project requires high resolution and high speed imaging. Re-positioning the reference path for hundreds or thousands of scans requires an infeasible amount of time. At this point in the project a hardware transition had to be made to a new OCT system.
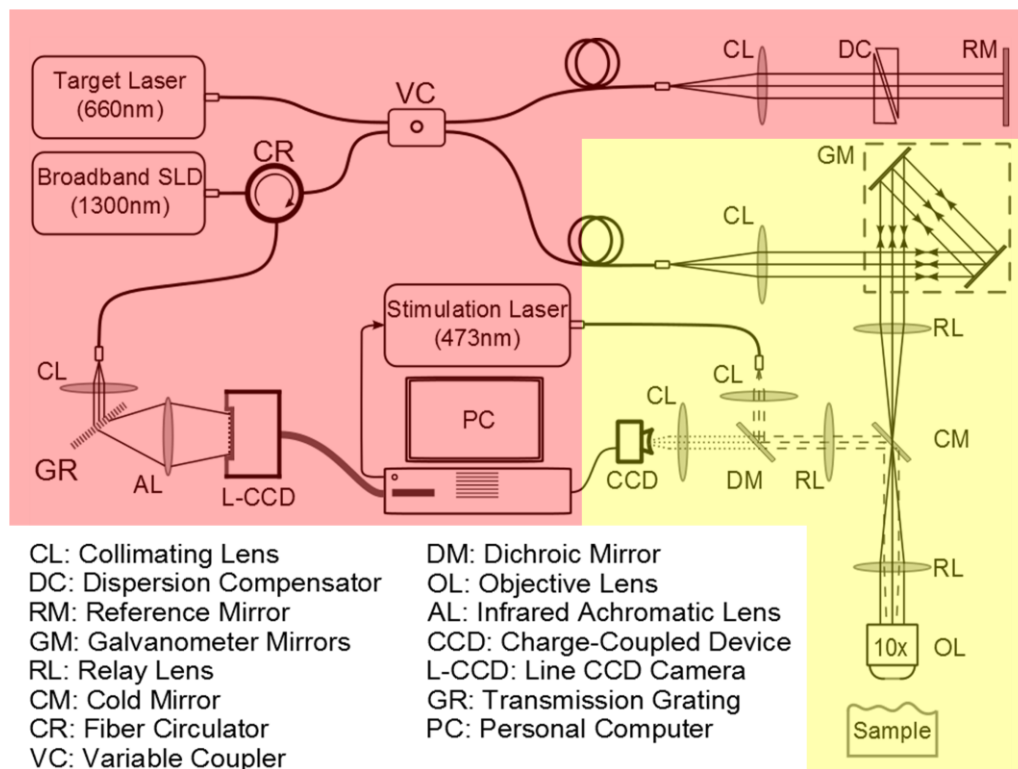
Figure 18: System diagram of SD-OCT system with table of components. OCT system separated into two major components, the source, detector and computer (highlighted in red) and the optical scanner (highlighted in yellow).

Spectral Domain Optical Coherence Tomography

In order to achieve the high speed imaging required by the project, a new Spectral Domain (SD) OCT system was built. The SD system designed, which can be seen in Figure 19,was divided into 2 principal components, the interferometer (highlighted in red) and the scanner (highlighted in yellow). Most notably, the new system does not require a moving reference path and instead

uses a spectrometer. The spectrometer can record the entire bandwidth of the low-coherent light source at each position along the surface of the sample. Instead of moving the reference path, the signal containing the interference pattern is diffracted through a transmission grating to open up the frequency spectrum [28]. The resulting spectrum is then focused onto a single line of 1024 (InGaAs) CCD detectors (Goodrich LDH2, inc). Since the speed of the system for each A-scan is now only limited by the camera exposure, time scans are now collected in factions of a second. The project is intended to achieve 'real-time' monitoring; the range of imaging speeds must therefore be between 20-40 cross-sectional images per second. In this case, 20,480 or 40,960 axial scans must be scanned and processed to display a 1024x512 pixel image in real-time. To achieve this, the new SD-OCT system was constructed.

Given that the primary component of the SD OCT is the spectrometer, one had to be added to the OCT system previously constructed. But before adding a spectrometer, it first had to be aligned and calibrated based on the transmission diffraction grating and the new light source. To improve the image resolution a new wideband source was used with the same central wavelength (1300nm) and 200nm spectral bandwidth (Thorlabs LS200B). Because the OCT source is using infrared light that is invisible to the human eye, a red aiming laser was initially used to align the central wavelength. Micro positioners, shown in Figure 20, were added to the grating and the camera mounting assembly for precise calibration of the system. Once the infrared light source was connected, the camera was aligned and calibrated first and then connected to the OCT system.
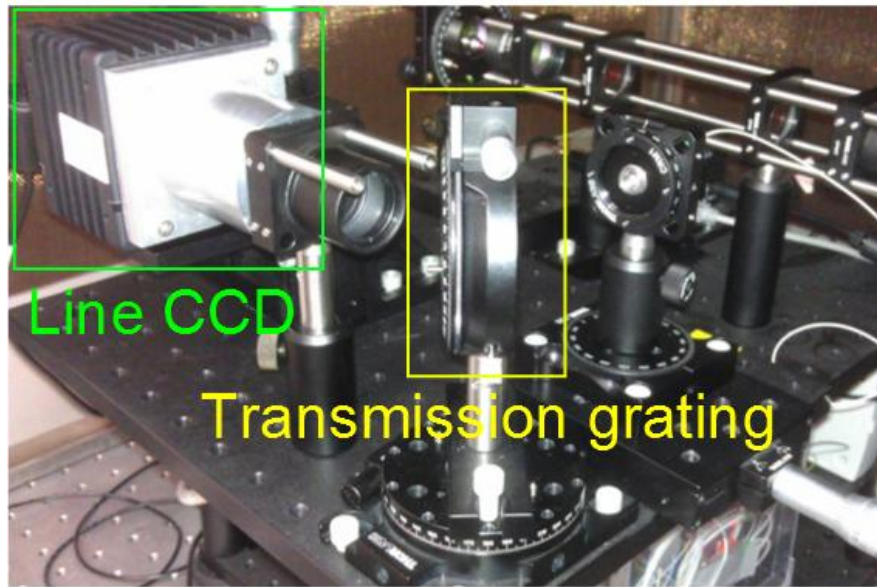
Figure 19: Image of spectrometer containing the line CCD and transmission grating mounted on micro-positioners

After the spectrometer was added to the OCT system the imaging acquisition speed increased dramatically, from 1 image to 20 images per second, leading to the final stages of hardware development. The next step was to add a cold mirror to integrate a CCD camera for bright field and fluorescent imaging into the OCT sample path. In the final step, a dichroic mirror was added to combine both imaging capabilities along with Optogenetic stimulation. To incorporate the new optics a mounting system was constructed. The 3rd and final version of the scanner was constructed and contained the optics for simultaneous sample imaging, scanning and Optogenetic stimulation. Again, the scanner was first designed and modeled in CAD (Figure 20) and then machined on the CNC. To improve the capabilities of the 3rd version, a retaining ring (see Figure 20) was added near the scan lens to reduce motion artifacts. The ring is pressed against a sample while scanning to help stabilize the sample with respect to the scanner.
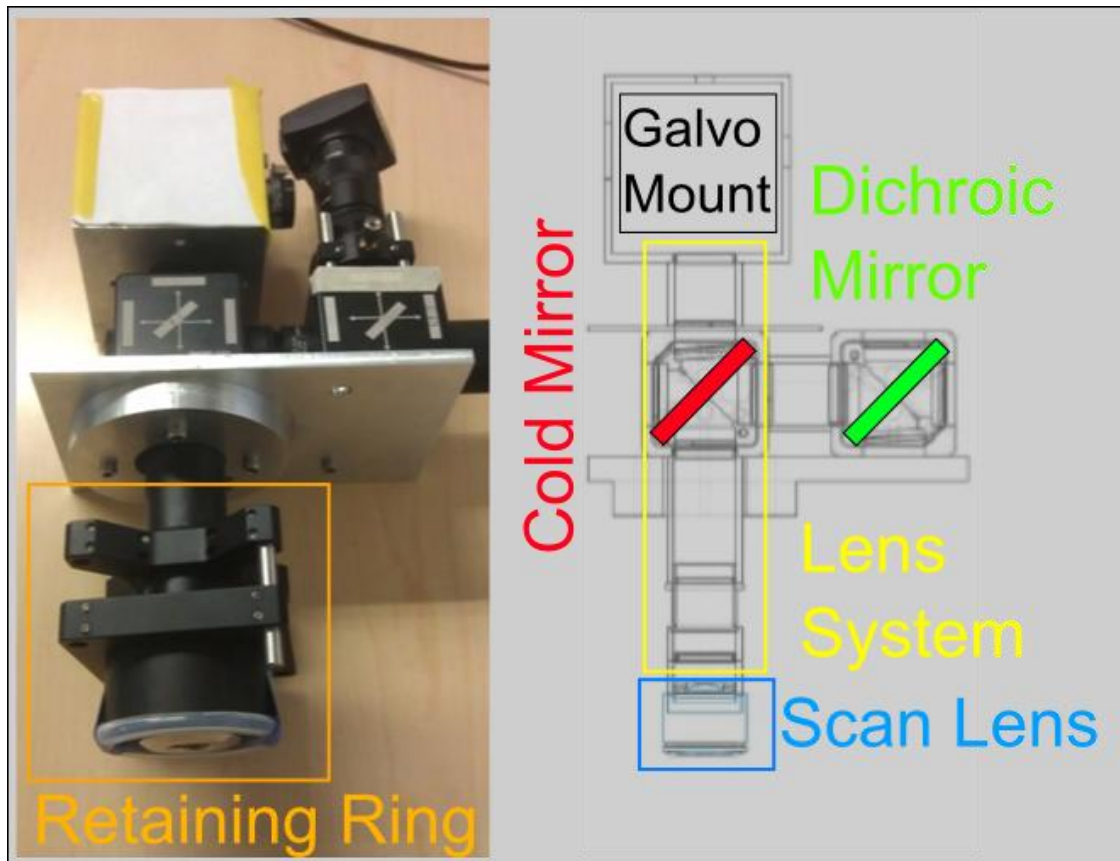
Figure 20: Image of final version of scanner head with attached retaining ring. The CAD diagram is show with the Cold mirror, Lens tube, Scan lens, Dichroic mirror and Galvo mount parts labeled.

Now using the new scanner head, the OCT system is divided into two major components. The low-coherent light source, interferometer and spectrometer are enclosed in a metal case that can be placed inside a cart. Finally, to improve the axial resolution of the imagesIn addition, a new light source was purchased with a wider bandwidth to improve the axial resolution of the images. The purchased dual source (Throlabs: LS200B) has a central wavelength of 1300nm and a bandwidth of 200nm. Utilizing the broadband source in conjunction with the new spectrometer, the new OCT system is now capable of recording the images of micro vasculature networks in the cortex.
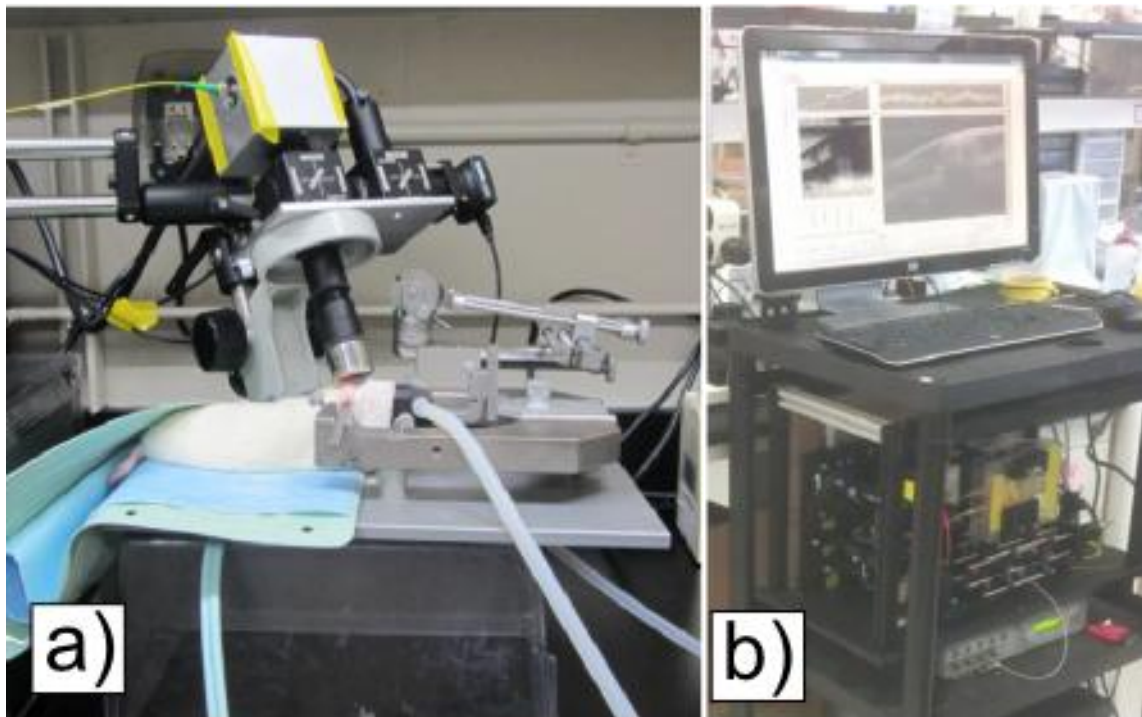
Figure 21: a) Image of SD-OCT scanner set up in animal surgery suit. b) Image of spectrometer, light source and interferometer with a computer monitor set up next to bench top experiment.

The new source is combined with the spectrometer and interferometer on a mobile cart that make up one half of the SD-OCT system. The other half is the scanner head which is mounted on a microscope double arm boom stand that is placed on a work bench or surgery table, seen in Figure 21. Additional computer hardware equipment is also inside the cart to operate the SD-OCT system and record the collected data. The mobile aspect of the OCT system takes the optical technology from the optics bench to *in situ* applications.

2.2 Software Design

Alongside the hardware development, the software to control mechanical systems and record the measurements had to be built as well. Before building the very first OCT system, the fiber based interferometer was manually controlled and the data was recorded via an oscilloscope. In order to create a more sophisticated, automated system, the Labview developer suite (National Instruments) was used. The development suite provides the tools to develop a user friendly graphic interface (Figure 22) as well as to control the hardware components. Using the developer software the initial graphical user interface was designed to move the reference path and galvos as well as record the interference signal. But as mentioned before, moving the reference path to each position and then scanning was very slow. The automation process improved the performance of the OCT system, but the speed was still limited.

When the transition was made to the SD-OCT, a second version of the Labview software had to be created. In the new version there was no more need to control the reference path while scanning. The major change in the software was acquiring the spectrum at each point on the surface of the sample. Moving the galvos and capturing interference spectra at first does not seem to be a major load on the software. But in the case of this project the goal was 'real-time' imaging, which requires 20,000 to 80,000 A-scans, or spectra, per second. The hardware, line CCD, data acquisition card and galvos, where all chosen to be capable of the required imaging speeds. The limiting factor is then the software because SD-OCT requires significantly more image processing than the former TD-OCT. The new Labview software had to include and run the essential image processing algorithms (which are explained in detail in the next section) in real-time.
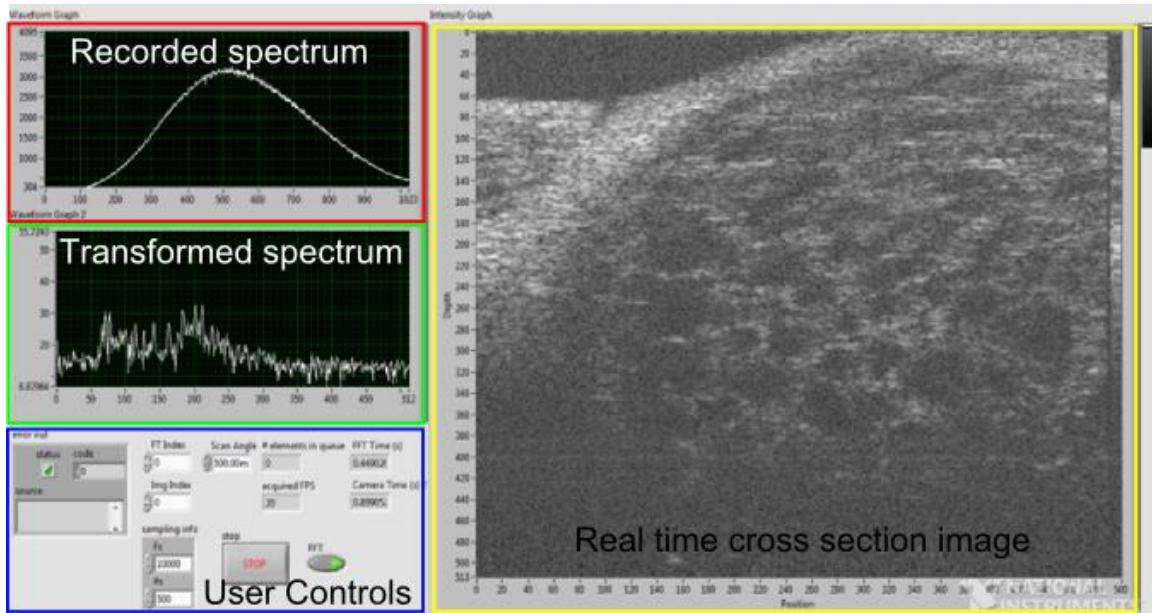
Figure 22: Screenshot of the SD OCT graphic user interface with real time cross section image and the corresponding recorded spectrum along with the basic user controls.

At first, simply encoding and adding the image processing algorithms was too much of a processing load on the Labview software. The software began lagging and the processed images were distorted or the program would simply fail to keep up. This problem was solved by combing new programming skills and a more efficient memory management algorithm. The image processing was taken off of the runtime Labview environment and converted to a C based language. The image processing was then compiled and wrapped in a Dynamic Link Library (DLL) which was then called by Labview. By pre-compiling the data and then calling it in the runtime environment, Labview was able to make more efficient use of its limited resources, in turn speeding up the monitoring software, such as the one in Figure 23.

In addition to the DLL, the amount of data being collected by Labview was more than the runtime environment could handle and crashed the software quickly. Since there is more than enough memory available on the computer, it was simply a process of moving data around more efficiently. The raw data was brought into Labview but then collected in a dynamic buffer right after being processed. The processed data could then be called from the buffer to be displayed on the monitor (Figure 23) or saved on the hard drive. After applying a few software modifications, the second version of Labview was able to image samples in real-time, or at 20 to 40 images per a second.
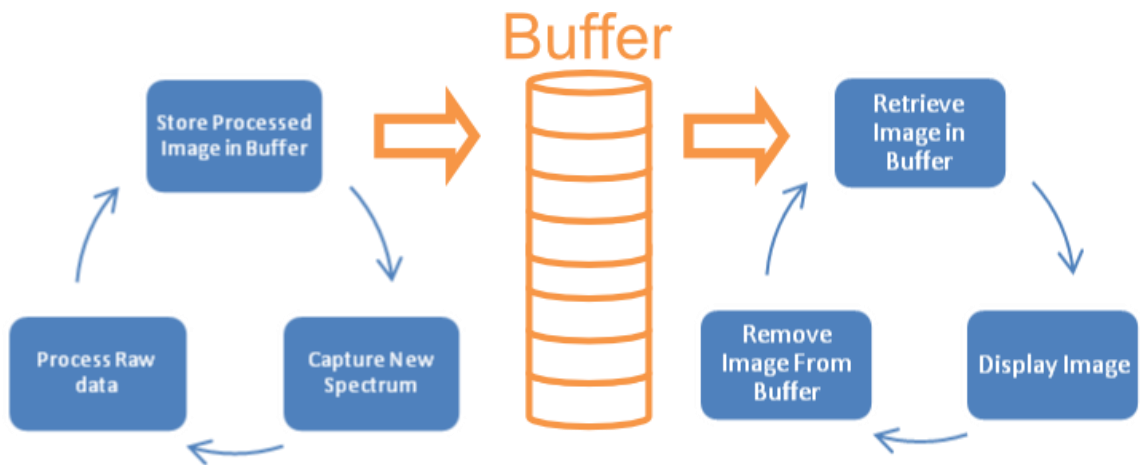
Figure 23: Diagram of memory buffer used to store scanned data before displaying on user interface.

Taking the next step in the software development of the system, a few more capabilities had to

be added. Because the goal of this project is monitoring real-time blood vessel changes in the

brain, new imaging methods had to be added to the software. OCT angiography and

velocimetery have been applied *in vivo* in brain tissue [29]. Two different DLLs were developed

to rapidly process velocimetery and angiography data to provide on-line processing, seen in

Figure 26.
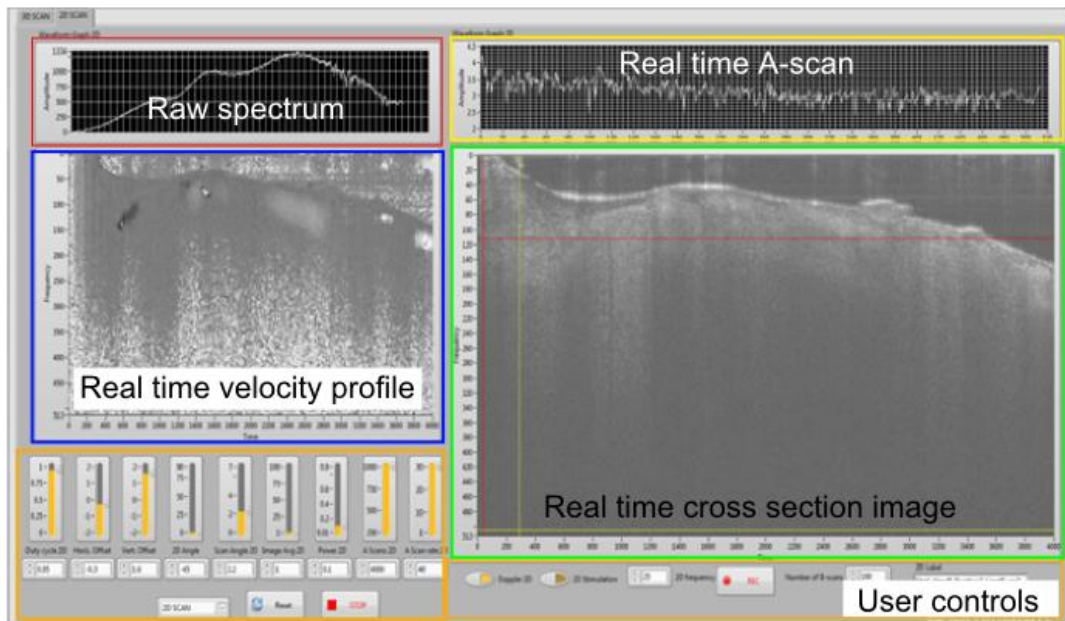
Figure 24: Final version of Labview user interface with real time cross section image and velocity profile along with simplified user controls to operate the SD-OCT system.

OCT angiography and velocimetery has been applied *in vivo* in brain tissue in post processing

[29]. A major goal of this project is to monitor the velocity of the blood vessels in real time. To

achieve this goal two different DLL were developed to rapidly process velocimetery and

angiography and display the data. The processed data is then displayed in the final version of

the Labview user interface, seen in Figure 26.

2.3 Image Processing

As previously mentioned, after the transition was made to the SD OCT system a new image processing technique and algorithm had to be developed and applied. In this section I will detail the process of how the recorded spectrum was processed and turned into the images seen in the results. Some of the image processing algorithms presented here are performed in Matlab (Mathworks, Inc.) or a C based language and some are performed in both. Since the raw data contains the spectrum of the inference patterns relative to position, the first step in processing the data will be transforming the raw data.

Cross section imaging

To transform the raw data from the frequency domain (the interference pattern), a multi step process is used to reconstruct an A-scan. At first the detected spectral domain is shifted when captured by the line CCD camera, requiring the spectrum to be re-sampled. Afterwards the spectrum is transformed into the time domain using the Fast Fourier Transformed in the West (FFTW) C++ library because of the algorithm's very high computation speed. Since the interference is a real signal the resulting signal in the time domain is symmetric around ZPD (zero frequency), so the mirrored signal is removed. A-scans obtained from different lateral positions are stacked together to produce a 2D cross-sectional image.
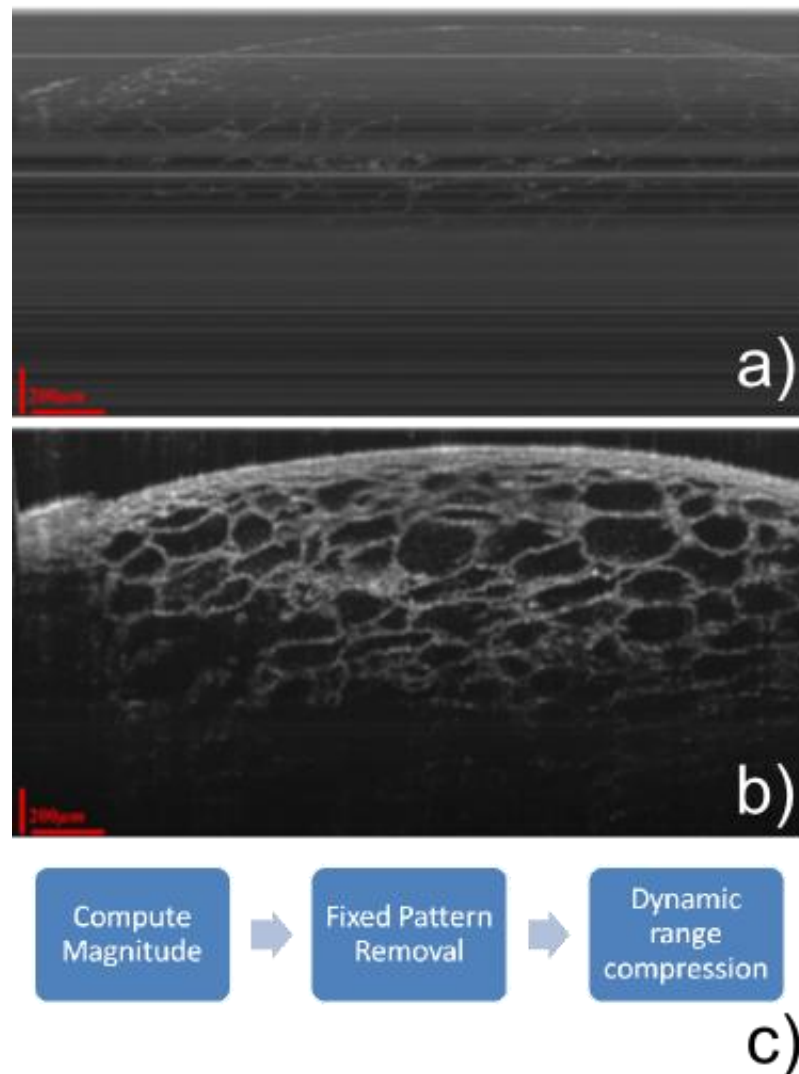
Figure 25: a) Cross sectional image of orange before background removal. b) Cross sectional image of orange after background removal. c) Image processing algorithm used to remove background from image.

Before displaying the cross sectional image, the sequential A-scans have to be processed as a

two dimensional image. Due to reflections from static parts of the OCT system (back reflection

from the fiber couplers, lenses, etc.) and/or noise pixel bias in the camera there is a fixed

pattern overlaid on the image. This background is constant across the lateral positions

estimated and varies across the axial position. Therefore the background noise is removed by

subtracting the average of all the image pixels at each depth, demonstrated in Figure 25. The

subtraction suppresses noise, helping to improve the signal to noise ratio (SNR). Since there is variability between A-scans in noise and noise removal, each magnitude can vary. To produce a more uniform image a magnitude computation must first be found followed by a fixed pattern removal. The resulting image's dynamic range is then compressed to produce a more uniform cross sectional image. Finally, the cross sectional image is displayed in the Labview software so that the user can monitor changes in the sample.

Velocity profiles (Doppler Imaging)

In addition to the real time structural monitoring, velocity profiles of moving particles or fluids also are displayed in the Labview software. Detecting and monitoring the velocity profile relies on the Doppler effect and is typically referred to as Doppler OCT. Since the detector is monitoring the spectral domain, a moving particle will produce a Doppler shift in frequency, the result of which will be a frequency shift on the detector. In order to record the shift in frequency, multiple A-scans must be performed over the same position on the sample. But because this creates a large amount of redundancies in the data, it was found that only 90% sample spot overlap is needed to detect the frequency shift. Therefore instead of recording form the same lateral position several times tissue was densely sampled such that there is 90% overlap between consecutive A-scans [30]. In addition it was also found that the scanning rate was proportional to the dynamic range of the Doppler shift that can be detected. Therefore for this project to monitor low velocity blood flow, low scanning rates must be used as well as vice-versa [31].
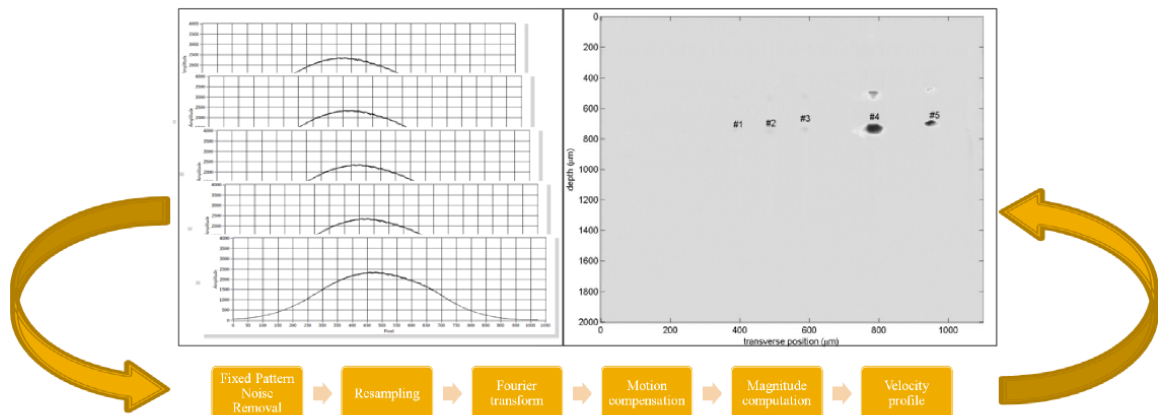
Figure 26: Diagram of multiple A-scans using a sequence of image processing algorithms to produce the velocity profile that is displayed for the user.

Angiography (Speckle variance imaging)

Beside the real-time processing, which is to help to target the desired area, data are saved into the hard drive for off-line processing and also to produce three dimensional images. The saved data contains the raw spectral information and are processed to produce a velocity map or angiogram of the tissue [32]. In order to obtain the tissue angiogram based on the speckle variance imaging, multiple recordings of a single cross section of the sample are scanned. Points within the cross section where the OCT signal changes between each scan indicate a moving particle where stationary structure does not change. Since the OCT system can perform high speed scans (up to 91,900 A-scans per second), 10 cross sectional images can be captured across the same position to improve the SNR and position accuracy. In a biological sample, due to breathing and heartbeat, there is motion in the tissue beside the motion caused by jittering of the galvo and OCT head micro movements. Before calculating the angiogram a motion

compensation algorithm was applied to reduce the motion artifacts and register consecutive B-scans recorded from the same position on top of each other. For velocity profile calculations a different strategy was used. First, motion between A-scans within a B-scan was compensated. Then the Doppler frequency shift for each pixel in the image was calculated [4] to obtain the cross-sectional velocity profiles. The cross-sectional velocity profiles obtained from different cross sections of the tissue were stacked together to produce the 3D velocity profile [33]. Both processing tools are used when analyzing the recorded data and allow for quantifying any changes observed in the blood vessels during the scans. Both angiography and velocimetery processes are implemented in the Matlab environment.
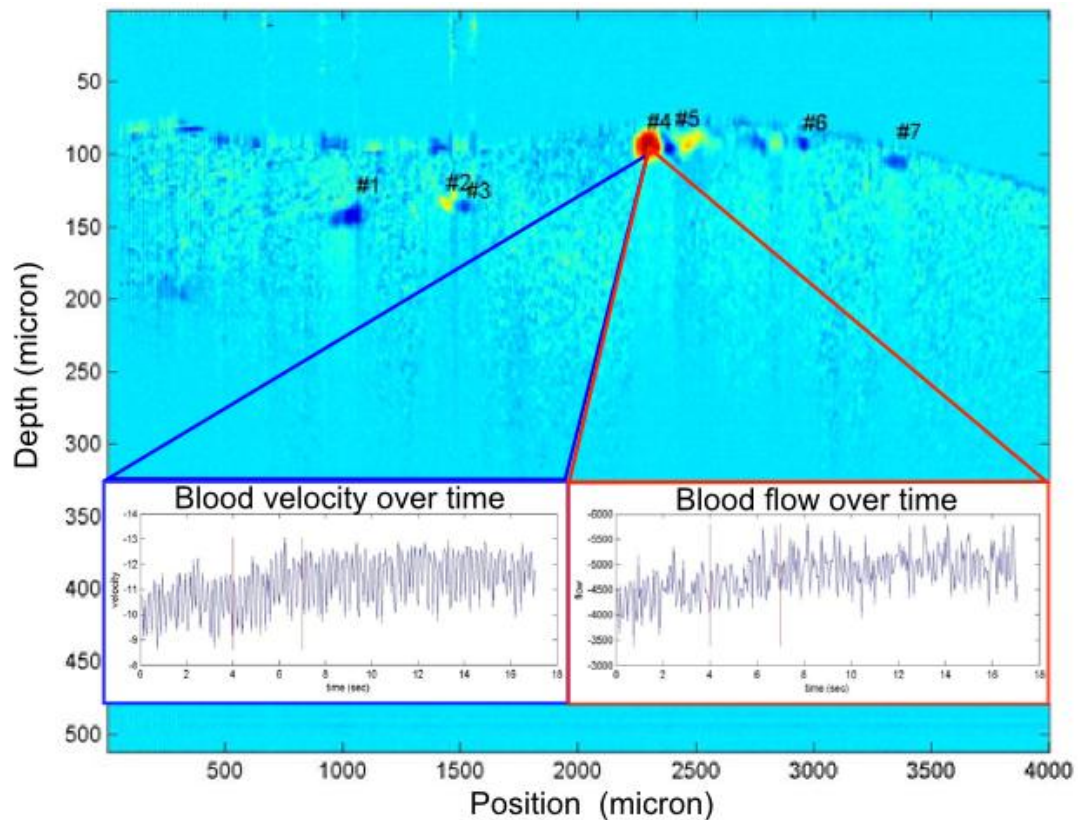
Figure 27: Cross section velocity profile with labeled blood vessels. Plots of blood velocity and flow are inserted of a selected blood vessel over time.

Velocity and Flow measurement

To quantify the velocity and the flow of the recorded blood vessels another post-processing

algorithm was developed in Matlab. The cross section images were fed into the program where

the velocity profiles where produced. A user then defined a region of interest (ROI) over a blood

vessel where the velocity was then calculated, seen in Figure 30. The algorithm finds the top

10% of the velocity values within the ROI over time. The process is repeated for each blood

vessel in the field of view. Velocity values for each vessel are then averaged at each point in time

and finally plotted over time. To measure blood flow a similar ROI is defined by the user but

instead of averaging, the product of the velocity and area are calculated. The result of this is the

blood flow which is then plotted over time to monitor hemodynamic response (blood velocity

and blood flow in vessels) after optical stimulation.

2.4 Experiment Method

We used the OCT system to image the cerebral blood flow and vessel diameter before and during neural stimulation. In this case the neural stimulation would be applied using the Optogenetics technology previously mentioned. Using this technology, neural activity could be stimulated with blue light (473nm) by activating the ChR2 in the cortex. This optical stimulation is applied through the OCT system so that the Labview software automates the entire recording and stimulation sequence. The 473nm light was generated by a fiber coupled laser diode (LaserGlow, inc) and collimated into the optical stimulation port on the OCT scanner. This allows for the optical stimulation of the corresponding field of view of the OCT imaging system since both use the same objective.

All procedures described were approved and conducted under the University of Wisconsin Madison Institutional Animal Care and Use Committee. To maximize the effect of Optogenetic stimulation, the decision was made to use transgenic mice (Jackson Labs Thy1-ChR2-EYFP H134R). The mice were genetically modified so that ChR2 was present in the entire cortex. Surgery was performed on the mice at first to remove the skull so that the OCT system had direct access to the cortex. But it was later found that the craniotomy caused severe trauma and hindered any results. Instead it was decided to thin the skull and install a cranial window for reinforcement. Thinning the skull instead preserved the hemodynamics of the cortex and reduced the trauma to the scanned tissue. After the mice were prepared with the thin skull window they were allowed to recover for 3 days. The mice were then scanned for approximately 1 hour under general anesthesia and then allowed to recover. Scans were then repeated again after 3 days of recovery and again the mice were allowed to recover afterwards.
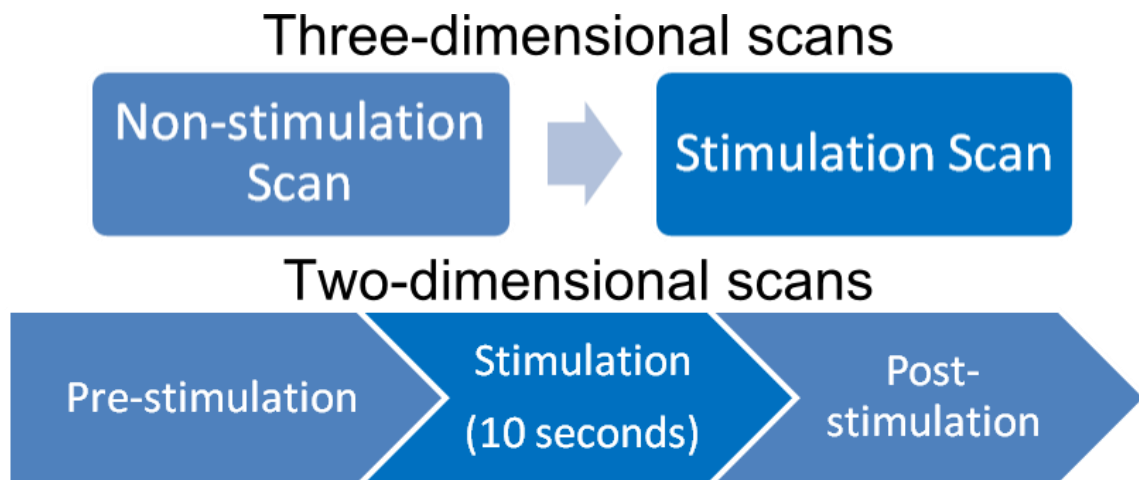
Figure 28: Diagram of scanning protocols used for three and two-dimensional scans.

Two scanning protocols were used for both the transgenic mice (n=5) and control mice (n=5) scans. The first of which, shown in Figure 31a, was the wide field volume scan, also called '3D Angio.' The entire field of view was scanned first without optical stimulation, and then repeated with optical stimulation. This scanning protocol was repeated multiple times on each mouse where each scan lasted between 1 and 2 minutes. The second scan protocol, shown in Figure 31b, targeted major blood vessels visible in the 3D Angio scans previously recorded. During the next scanning session a cross sectional velocity profile was scanned, also called '2D Doppler' for up to a 40 second time period. Optical stimulation was applied after 5 seconds over a duration of 10 seconds. The data was recorded and then saved to the hard drive for analysis.

Chapter 3: Results from simultaneous optical neural stimulation and hemodynamic monitoring

This chapter will focus on the results obtained during the optical stimulation and imaging experiments performed. To achieve the proposed goals of the project the results must be able to demonstrate the following characteristics. First to identify hemodynamic changes, such as blood vessel dilation, the networks of blood vessels and capillaries must be recorded. Second to monitor changes in the velocity and flow of the blood, a velocity profile must be captured as well. Finally, the changes observed must be quantified over time to compare the hemodynamic changes with Optogenetic stimulation.

 In the first round of experiments, which used the open skull technique, results were collected and analyzed using the image processing techniques described in Chapter 2. Between the two rounds of experiments a thin skull technique was tested and then implemented for the second round. In the second round of experiments the same optical stimulation and imaging experiments were performed using the thin skull technique.

The results presented will consist of cross section images, velocity profiles, volumetric images and velocity measurements over time. Each of which provides a different view point of the effect created by the Optogenetic stimulation. In the cross section images and velocity profiles changes in diameter and velocity can be easily observed over time as a blood vessel cross sections dilate over time. The volumetric images, also called 3D Angio or 3D Doppler, are

recorded and then projected onto a plane to study the wide field effect of Optogenetic

stimulation within the field of view of the scan. The last tool that will be used is the

quantification of the blood velocity and flow. The output will provide measurements over time

which will be correlated with the application of Optogenetic stimulation.

3.1 Open skull imaging

In the first round of experiments an open skull scanning protocol was used. Using this technique, a craniotomy was first performed on the animal. After the skull had been removed both 3D Angio and 2D Doppler scanning protocols where used. The 2D Doppler scanning protocol was used first on the major arteries and veins in the field of view. Multiple scans were taken at each site, and multiple sites were scanned. Afterwards, the 3D Angio scans were performed on the field of view where multiple scans were taken to validate the repeatability of the results.

A single cross sectional image of a processed speckle variance image, which is sometimes referred to as an Angio. A sequence of cross sectional Angio images is collected over the volume of the sample as seen in Figure 5. The sequence of cross sectional images is then stacked to create a 3D volume image. The 3D image is then projected onto a pane so that it can be visualized as a 2D image, as seen in Figure 29.
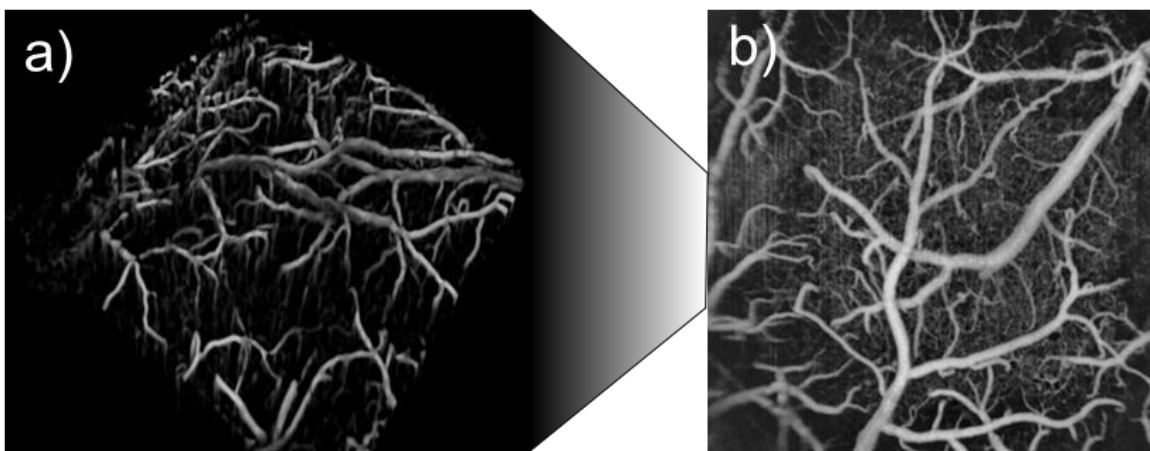
Figure 29: a) Three-dimensional angiogram. b)Projection of angiogram onto two-dimensional plane.

The anticipated outcome was to observe similar changes in blood vessel velocity and dilation as seen in previous studies (CITE DMD). Based on the results that were recorded, changes in the blood velocity and vessel diameter were observed. At first only small arterioles were observed to change diameter with and without stimulation. After further analysis of data it was observed that the larger blood vessels were dilating as well. The changes are indicated by the red circles and arrows in Figure 34 where the blood vessels increase in diameter with applied stimulation.
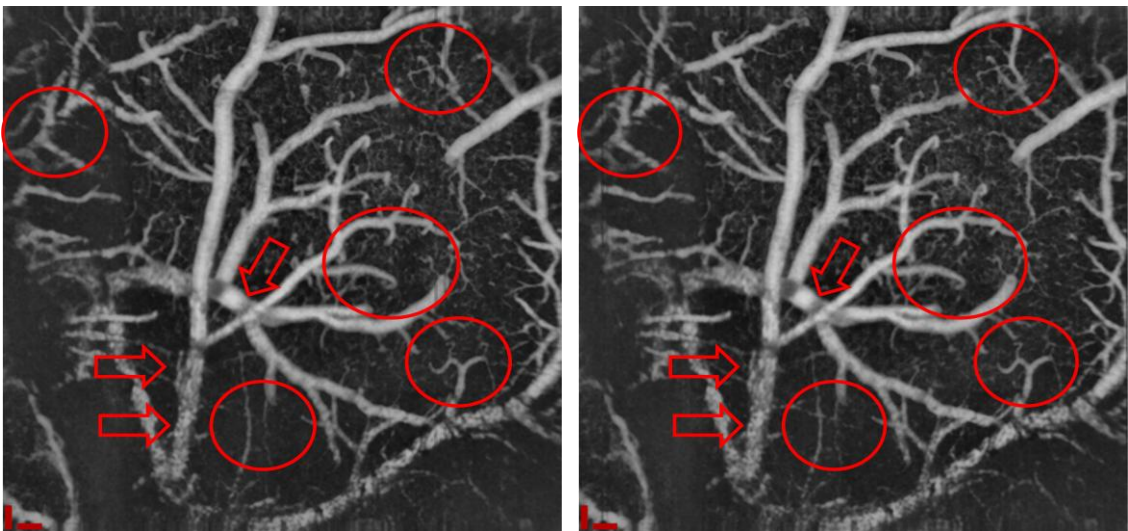
Figure 30: Angiograms with red indicators of changes observed between no optogenetic stimulation (left) and with optogenetic stimulation (right), (0.1 mm scalebar).

In addition to the Angio images, a three-dimensional Doppler scan was also taken to identify wide field changes in blood velocity. Changes in the velocity were seen relative to the sites of dilation in the Angio image above. To better correlate the changes in the Angio projection and velocity profile, the two images were superimposed onto each other. Also note the red to green transition along the blood vessel. The change in color is due to the positive or negative angle relative to the OCT system. Combining the two images has the capability to find wide field

changes in blood velocity and blood vessel dilation. Sites where changes in both dilation and

velocity were detected are indicated in Figure 30 by red circles and arrows.
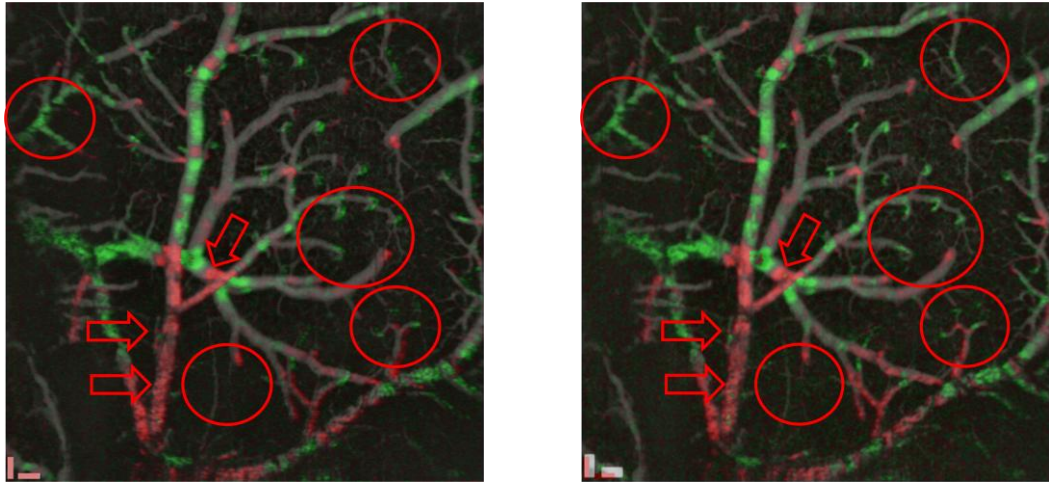
Figure 31: Angiogram projection with velocity profile overlay. Projections with red indicators of changes observed between no optogenetic stimulation (left) and with optogenetic stimulation (right) (0.1mm scalebar).

Along with the wide field 3D scans that monitored changes from a view point above the brain,

the 2D scans recorded data from a different point of view within the brain. Changes in blood

velocity and flow were seen in the cross section scan of the cortex. Increases in diameter and

velocity were measured using a velocity profile such as in Figure 31. By comparing the cross

sections with and without Optogenetics stimulation, changes in the diameter can be observed.

To quantify the measurements taken in the cross sectional scan, blood vessels first must be

labeled and then processed. As described in the previous chapter, an ROI is placed over a blood

vessel, where it is then indexed and processed by the Matlab software. The changes in velocity

and flow are first averaged over 5 different scans and then plotted over time. The results of

which can be seen below, in Figure 32, where the blue lines represent the point where

Optogenetic stimulation is applied and the resulting changes are observed.
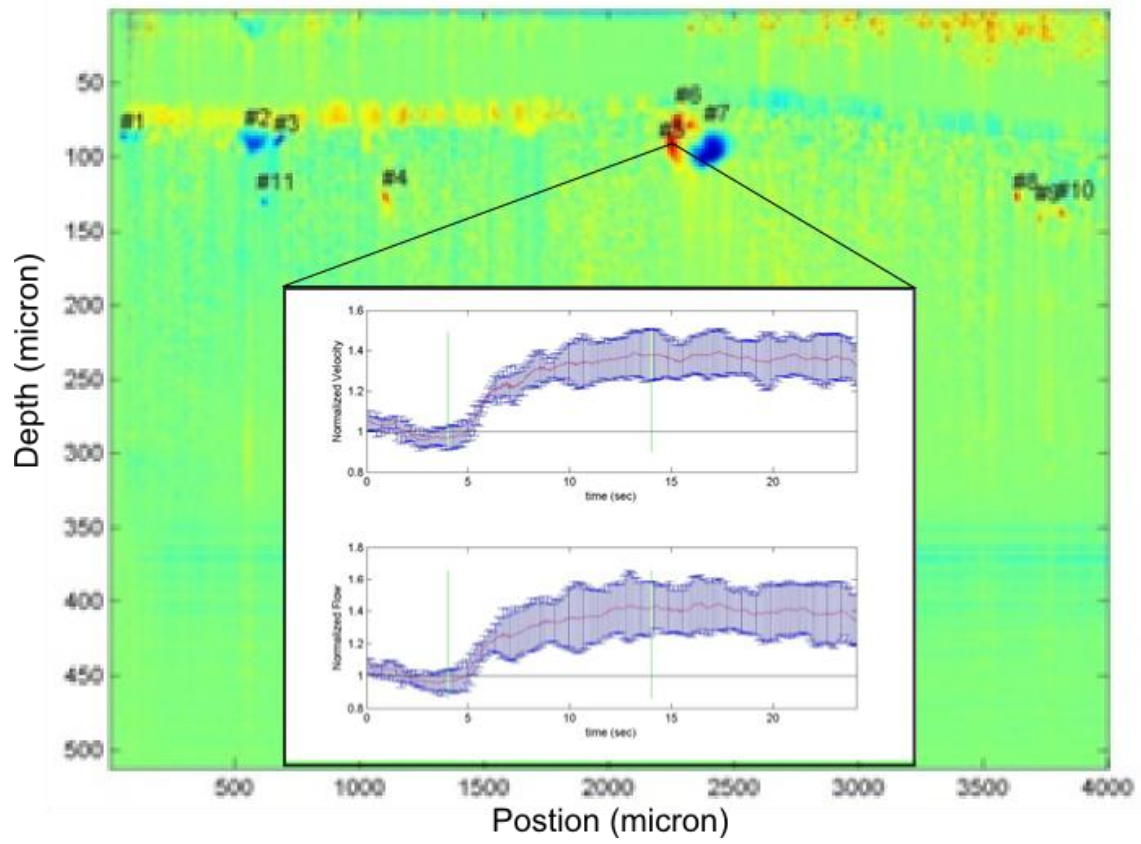
Figure 32: Cross section velocity profile with individual graph of selected blood velocity and flow over time.

3.2 Cranial Window

After the first round of experiments the changes in blood vessel dilation and velocity seemed to have been dampened compared to previous studies (CITE DMD). It was proposed that the open skull experiments were causing too much trauma to the cortex. The trauma would then have already changed the hemodynamics of the blood vessels and in turn dampened the anticipated results. To resolve this problem it was then decided to reduce the trauma to the brain by thinning the skull instead of removing it. In a thinned skull experiment, the thickness of the skull was reduced using a burring tool and then applying a thin glass cover slip for reinforcement [34]. A graphic demonstrating the thinned skull technique can be seen in Figure 38a, but no water or water dipping objective was used in this case [35]. Because of the addition of the glass in the sample path, an equal distant glass compensator must be installed in the reference path. Testing of the thinned skull technique was performed on 4 rats and 1 mouse. The first experiments were performed to both test and verify the ability of the OCT system to image through the thinned skull and glass window. In addition, Angio and velocity profiles (Figure 38b) were also recorded to test for any variations the thinned skull and window might produce.
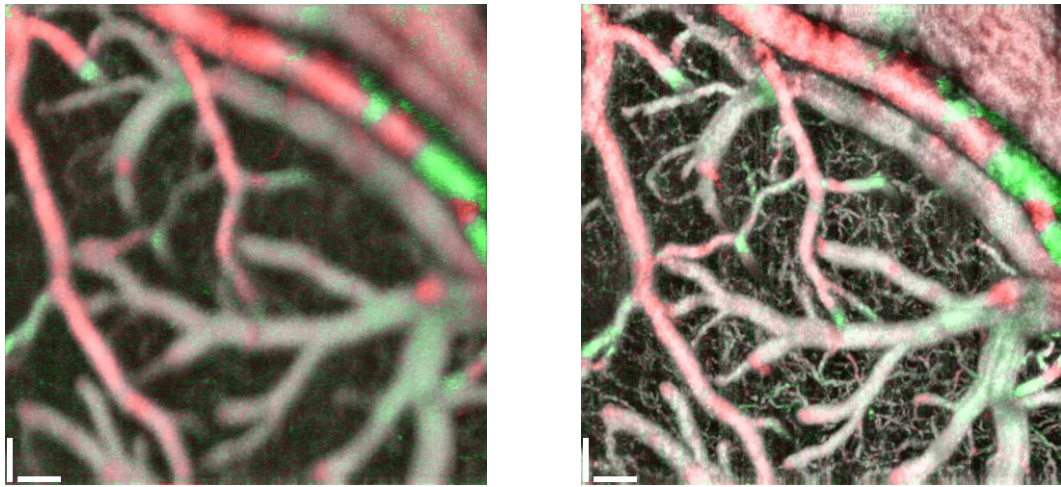
Figure 33: Angiograms with velocity profile with cranial window comparing images taken without a compensator (left) and with a compensator (right).

3.3 Thinned skull imaging

In the second round of experiments the thinned skull surgery was performed on 5 mice (2 ChR2, 3 Wild) and they were allowed to recover for at least 3 days. After the recovery period all five mice were scanned over a two day period. Over the two days, multiple 3D Angio and Doppler scans were performed over the entire field of view. Total measured optical power at the focal point of the Scan lens was 12mW, which was the same as previous experiments. With the skull still intact and after 3 days of recovery, no noticeable trauma could be seen above or below the thinned skull.

The same scanning protocol as the first round of experiment was followed, both without stimulus and with Optogenetic stimulus scans. Using the thinned skull technique, the blood vessel dilation was much more noticeable in comparison to the first round. In Figure the red ROIs highlight the dilation of the larger blood vessel within the field of view. All ROIs are along the same blood vessel, which indicates that the Optogenetic stimulation is triggering a response. The dilation also confirms results that were previously seen.
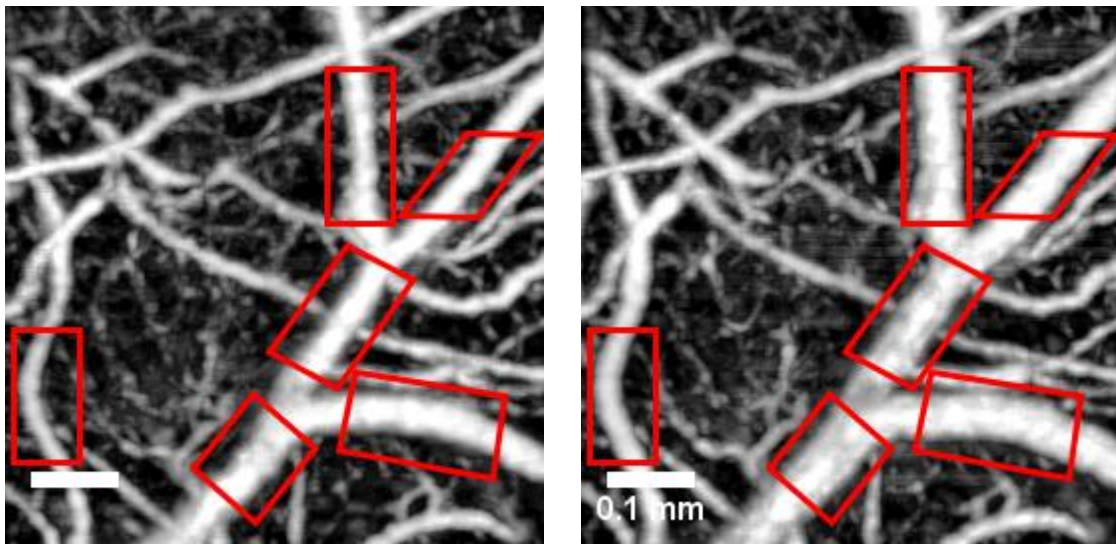
Figure 34: Angiogram without and with Optogenetic stimulation with red ROIs over blood vessels that dilated following optogenetic stimulation.

Along with the 3D Angio scan, velocity profiles were also taken from the same field of view. The velocity profile provides another tool with which to monitor the changes occurring with Optogenetic stimulation. In Figure 39, the 3D Doppler images demonstrate both the dilation as well as the increase in blood velocity with Optogenetic stimulation. Some points in the velocity profile switch from red to green or vice-versa, which may indicate one or two things. The first of which may be that the blood velocity is inverted because it increased above the highest detectable velocity. The second may be that the blood vessel itself has dilated and re-oriented itself with respect to the OCT system, causing the change in color. To further study the change in velocity, flow and dilation of the blood vessel a cross sectional image was taken afterward.

Pre Stimulus   Intra Stimulus

>7mm/s

200μm   200μm

<-7mm/s
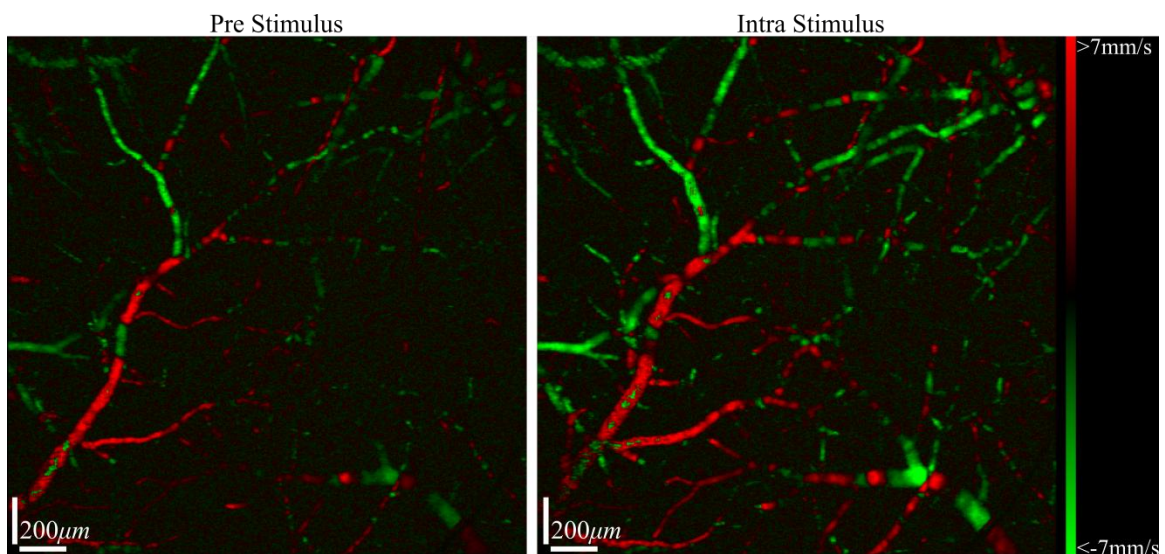
Figure 35: Velocity profiles pre and intra optogenetic stimulation where the increase in velocity is observed as well as the dilation of blood vessels.

After the initial 3D scans performed on the mice during the 2 day period, the mice were allowed

to recover and rest for 2 days. For the next scans all 5 mice (2 ChR2, 3 Wild) were scanned again,

this time using the continuous 2D protocol with a 10 second intermediate stimulation.

Optogenetic stimulation was applied after a 5 second baseline was recorded. Following the 10

second stimulation period a 25 second recovery period was recorded. As seen in Figure 40, the

blood vessels dilated and the velocity increased with stimulation. The effect can be seen in the

cross section images in Figure 40 where the velocity is color coded.
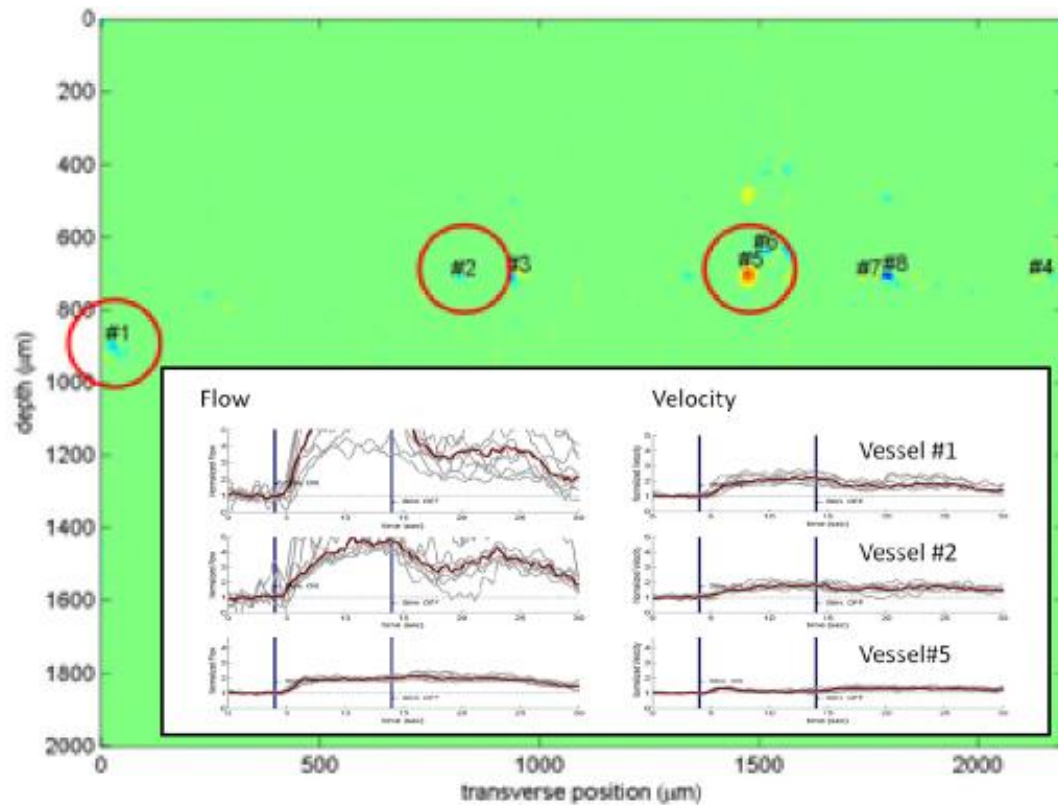
Figure 36: Quantitative velocity and flow measurements of selected blood vessels in cross sectional velocity profile image

To again quantify what was observed in the Angiograms and cross sectional images, measurements were taken. An ROI was placed over the 3 circled blood vessels in Figure, and each was processed using the Matlab software as described above. The results of the analysis show an increase in blood velocity only seconds after stimulation. When comparing the velocity and flow, the dramatic increase in blood flow corresponds directly with the sudden increase in velocity. Since flow is determined by velocity and cross sectional area, and the velocity remains somewhat constant after the initial increase the rapid increase in flow is more likely due to the rapid dilation of the blood vessel. A rapid dilation of the blood vessel wall is a result of smooth muscle control and neural activity, which has also been previously reported [23].

3.4 Wild type imaging

In addition to the ChR2 mice, Wild type mice were also used as a control group. The Wild type mice express no indication of the presence of the ChR2 gene. Without the gene, the mice will not be subject to any neural stimulation when the Optogenetic stimulation (blue light) is applied. The purpose of this control is to rule out any thermal or heating effects. Control experiments were performed in both open skull (n=2) and thinned skull (n=3) rounds of experiments. The same scans and scanning protocols where performed on all ChR2 and Wild type mice. After recording and analyzing the results from the Wild type experiments, no significant changes in blood vessel velocity or dilation were observed. The point in time where optical stimulation was applied is indicated again by the blue vertical lines in Figure 37. Minor changes, i.e. less than 10%, were observed in all ChR2 and Wild type mice and are considered to be background fluctuations.
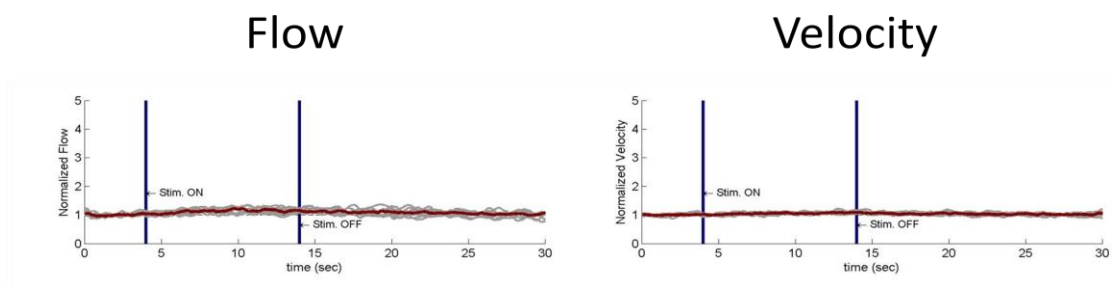
Figure 37: Characteristic blood flow and velocity measurements taken from wild type mice
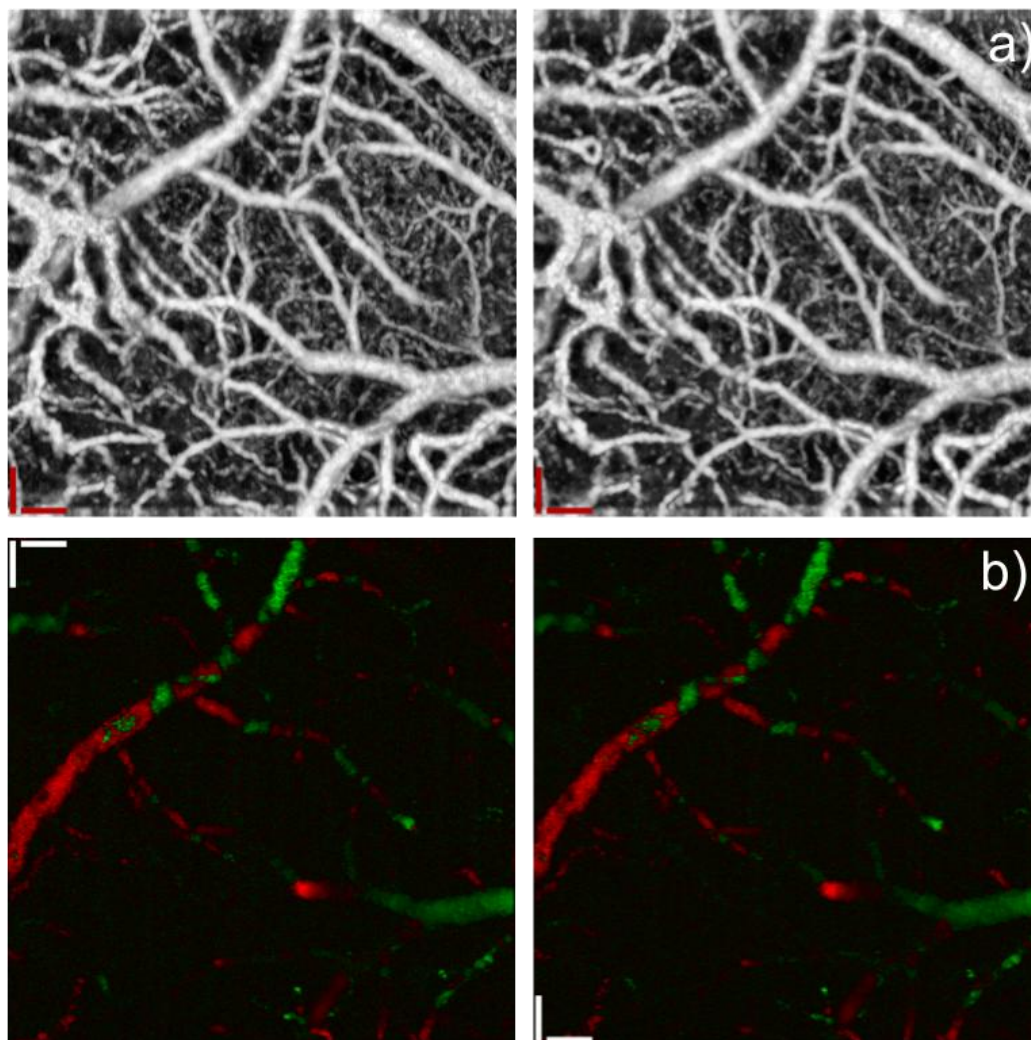
Figure 38: a) Angiogram of control mouse without (left) and with optogenetic stimulation (right). b) Velocity profile of control mouse without (left) and without optogenetic stimulation (right).

Again, to confirm no significant changes where occurring with optogenetic stimulation, scans were recorded using the same scanning protocol as before. In the Angiograms and velocity profiles in Figure 38, comparing without and with optical stimulation, no noticeable changes where observed. Results from the control mice all indicated no variation from the observed background with optical stimulation as the Velocity graph in Figure. The greatest fluctuation in flow for all control animals seen in Figure, still remains within the background fluctuations.

3.5 Summary

Based on the data collected this project has demonstrated the capability of monitoring hemodynamics while stimulating neural activity. Two rounds of experiments were performed, the first using an open skull technique. The second round used a reinforced thinned skull technique which reduced trauma and allowed for a healthier animal recovery. The OCT system was able to confirm that the increase in neural activity leads to an increase in blood velocity and dilation. No significant changes in either blood velocity or dilation were found in any control animals. The results of this project suggest that the increase in blood velocity and dilation are a result of neural activity.

Chapter 4: Functional imaging with Optogenetic stimulation

In this chapter the focus will be a project that combined Functional Magnetic Resonance with Optogenetic stimulation. The overall goal was to stimulate neural activity deep in the brain and monitor the resulting Blood Oxygenation Level Dependent (BOLD) signal. The project aimed to achieve the following essential goals to provide proof of concept. First of all, a method was developed to deliver optical stimulation to an animal inside the MR scanner. The second was to gather evidence of neural activity and the characteristic BOLD signal. Finally, using collected data, the hemodynamic response function of Optogenetic stimulation was calculated.

Simply stated, to provide proof of concept a method must be established to stimulate neural activity with Optogenetics. In order to achieve this goal, optical stimulation hardware had to be customized to operate inside the MR scanner. The optical stimulation has to be delivered precisely through software automation which must also synchronize with the MR scanner. Before running experiments, a scanning protocol must also be established so that each scan is comparable.

The results of the scans were then used to validate the Optogenetic stimulation of neural activity which in turn will produce a BOLD signal. The first method to validate functional activity was correlating Optogenetic stimulation with electric stimulation. The second one was applying different stimulation durations and amplitudes. Finally the third was finding the Hemodynamic Response Function (HRF) of both the electric and optical stimulation. The HRF provides a metric used to monitor functional activity [36] . The results of this project demonstrate the

confirmation of all of the above conditions. In the end the three strong indicators observed

provide a proof of concept that Optogenetic stimulation can be monitored by fMRI [37] [38] .

4.1 Hardware customization

This project was inherently challenging due to many technical factors surrounding the MR scanner. In order to begin this project the first step was to gain access to the fMRI scanner, available at the Medical College of Wisconsin. Once that was achieved it was time to develop the hardware and mechanisms to perform the study. Since the MR scanner produces a very strong magnetic field all of the components in or near the magnet must not be paramagnetic. Most of the challenges that will be discussed regarding this project were based on designing or customizing the system so that it could operate in or around the MR scanner.
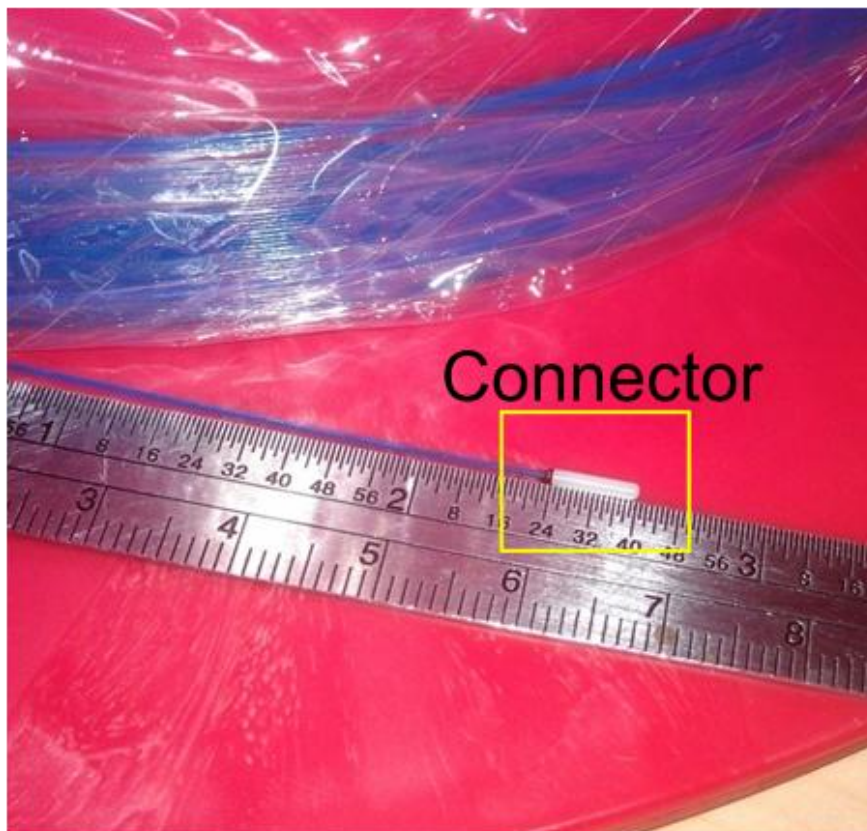
Figure 39: Optical fiber with custom ceramic connector.

The first challenge in order to incorporate Optogenetics into an fMRI system was optically stimulating the brain while it was inside of the MR scanner. To solve this fiber optics were used to send light from a laser into a fiber optic probe inside the brain. The fiber optic probe is precisely inserted into the brain using sterotaxis surgery techniques [39]. In order to implant a fiber optic probe a ceramic connector had to be fixed to the skull. To reduce the chance of creating artifacts in the images, a small ceramic connector (1.25 mm diameter) was used (Thorlabs Inc). The connector could then be coupled with a 200 μm core optical fiber that would allow for the optical stimulation to be delivered into the brain. Because of the strong magnetic field, the source of the optical stimulation, the 100mW 473 nm laser (LaserGlow, Inc), had to remain outside the MR scanner room. A 20 meter fiber optic patch cable with a custom ceramic cannula (Figure 39) runs from the MR scanner to the laser and is used to deliver the optical stimulation to the probe (Figure 40).
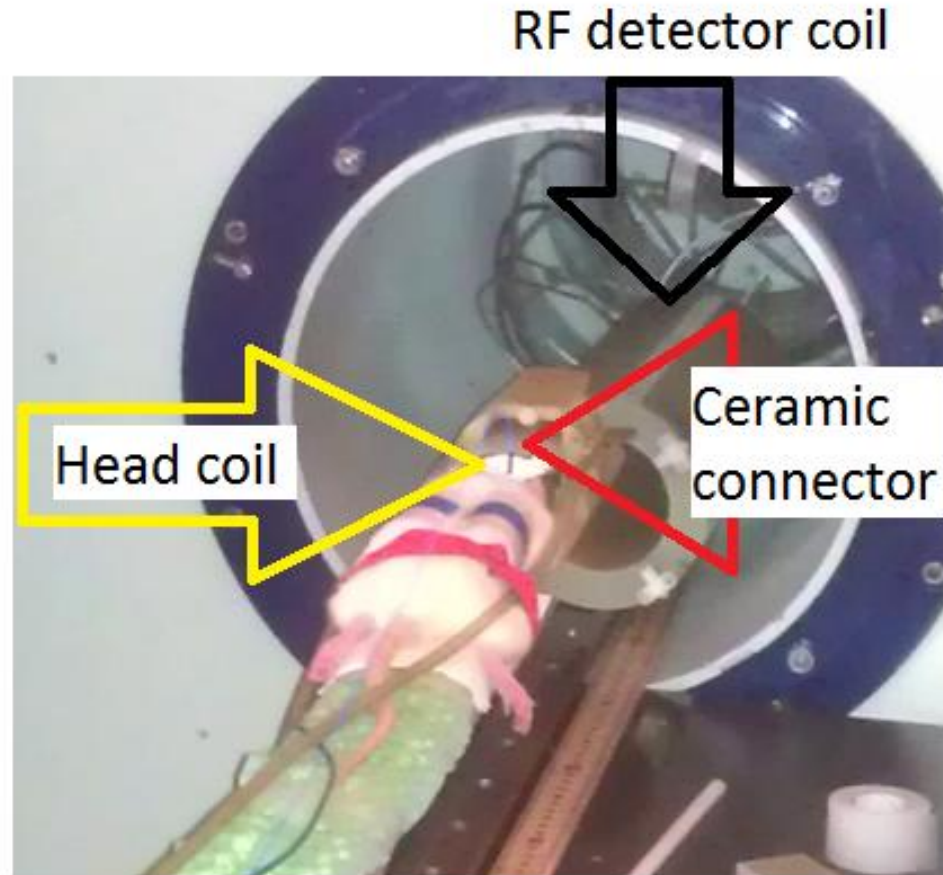
Figure 40: Animal on MR scanner gurney with modified head coil and optical fiber connector. The animal and custom components all must fit inside of the RF detector coil in front of the animal.

The fiber optic then had to connect to the probe inside of bore of the MR scanner. Because space was limited the fiber's protective wrapping had to be removed to allow for more mobility. Without the wrapping the fiber could make a 90 degree bend inside the bore. By customizing the hardware components and making the optical stimulator more remote the first challenges were resolved.

4.2 Software Development

The next step was to synchronize the optical stimulation with the functional imaging. To do this the optical system had to be automated and interact with the MR scanner system. Both of these attributes are necessary to achieve the overall project goals. Automating the systems will synchronize the stimulation and scanning times to allow for more accurate measurements. To achieve these goals software was developed in the Labview environment to interact with the MR scanner and control the optical stimulator.

To automate the system the Labview software was developed to control the 473 nm laser that provides the optical stimulation. The user interface of the software (Figure 41) provides the user all of the necessary controls to set up an automated Optogenetic MR scan. In Figure 45 the user inputs the stimulation amplitude, frequency and duration of the optical pulses. In addition the user can also set the pre and post stimulation time interval to allow for a rest period between scans. Since fMRI scanning sequences usually require multiple repetitions, the user can also set the software to repeat a set number of iterations, typically 3 to 5 repetitions. After all of the parameters are set, the system enters the run state and will begin when the start button is pressed. The software controller's ability to automate the optical stimulation helps maintain the timing accuracy for future data analysis.
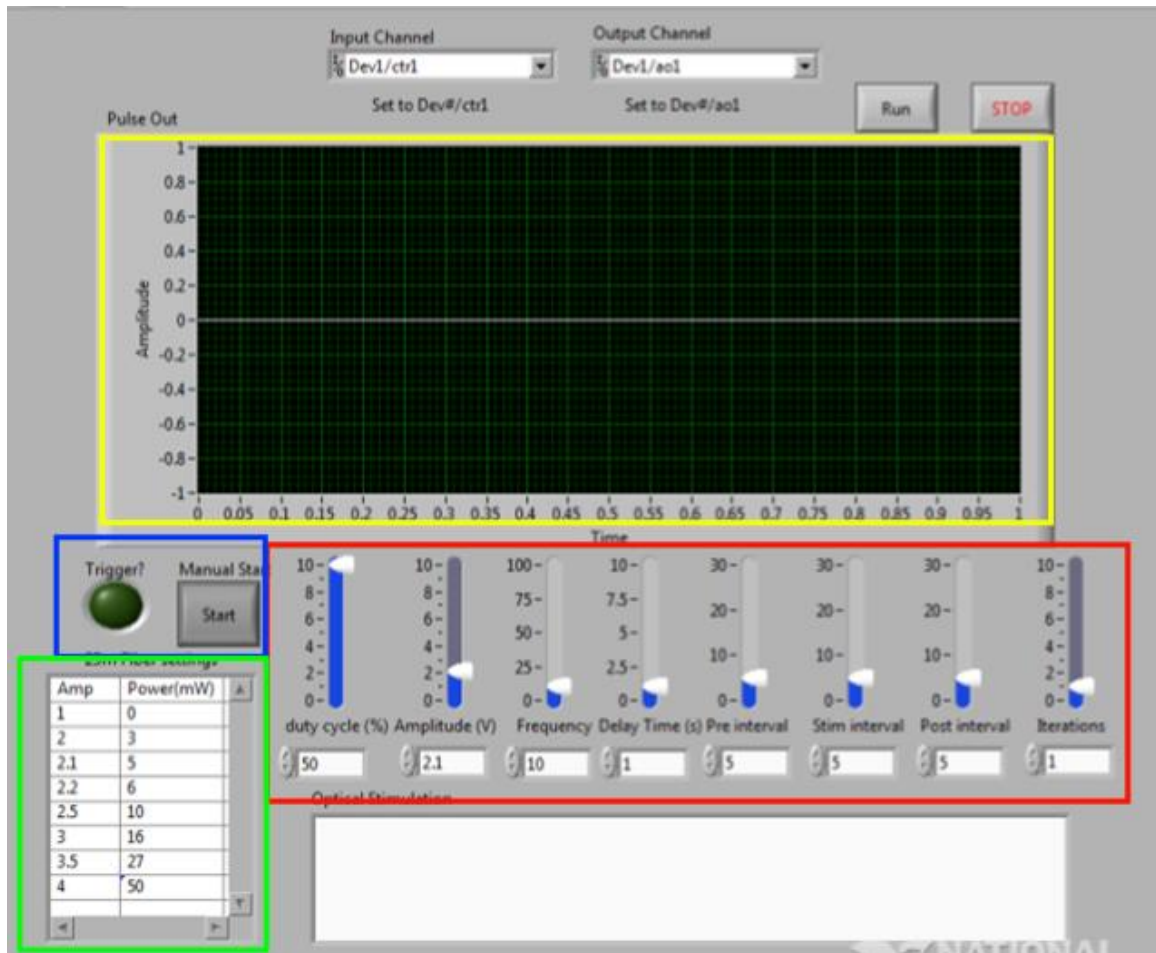
Figure 41: Screenshot of user interface of optical stimulator controller. Yellow box: Graph of optical stimulation pattern. Red box: Stimulation parameter controls. Blue box: MR scanner synchronization monitor. Green box: Calibrated settings for optical power output.

With the Labview software able to automate the optical stimulation the system now has to be synchronized with the MR scanner. Since the accuracy of the MR scans is dependent on time, the stimulation must be applied at precise points during the scan. Because the optical stimulation and the electric stimulation are two separate systems that do not interact with each other, the MR scanner is used as a common reference point. To synchronize both the optical and electrical stimulation an initial sync trigger is generated by the MR scanner. The trigger, demonstrated in Figure 42 is detected by both stimulators and the automated sequence begins.

As of now only one stimulation modality is used at one time, but the option of combining both is possible if desired in future projects. Using the MR scanner as the reference point the data generated with both stimulation modalities can be compared side by side.
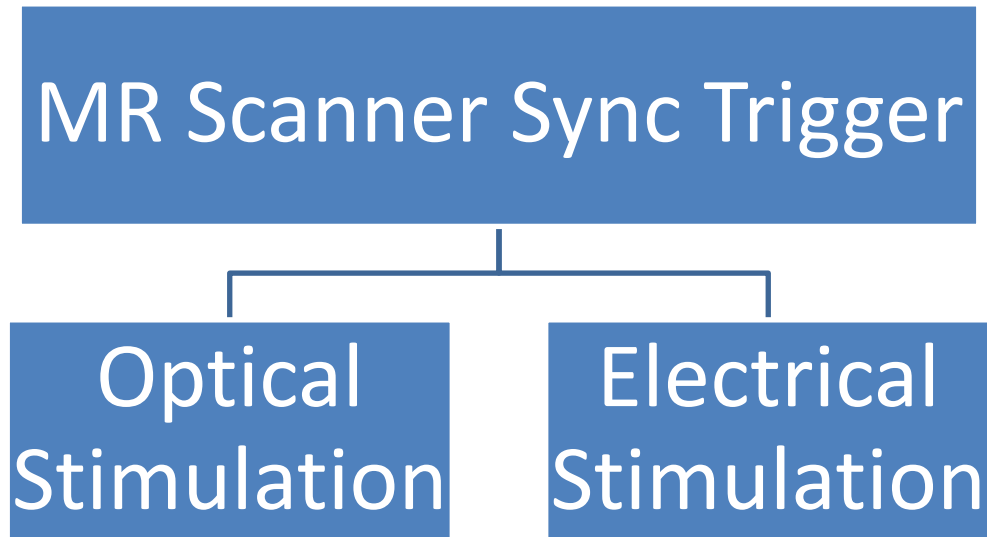
Figure 42: Diagram of MR scanner synchronization scheme.

4.3 Experimental Protocol

In order to perform the high quality measurements required by the project, a well defined protocol was established. To minimize any error a sequential protocol was settled upon (Figure 47) and repeated in order to perform high quality and repeatable results. Before the protocol was in place results varied from scan to scan. But after trial and error, the protocol currently in use was established. The data collected using the current protocol has been repeatable and reduced sources of error.
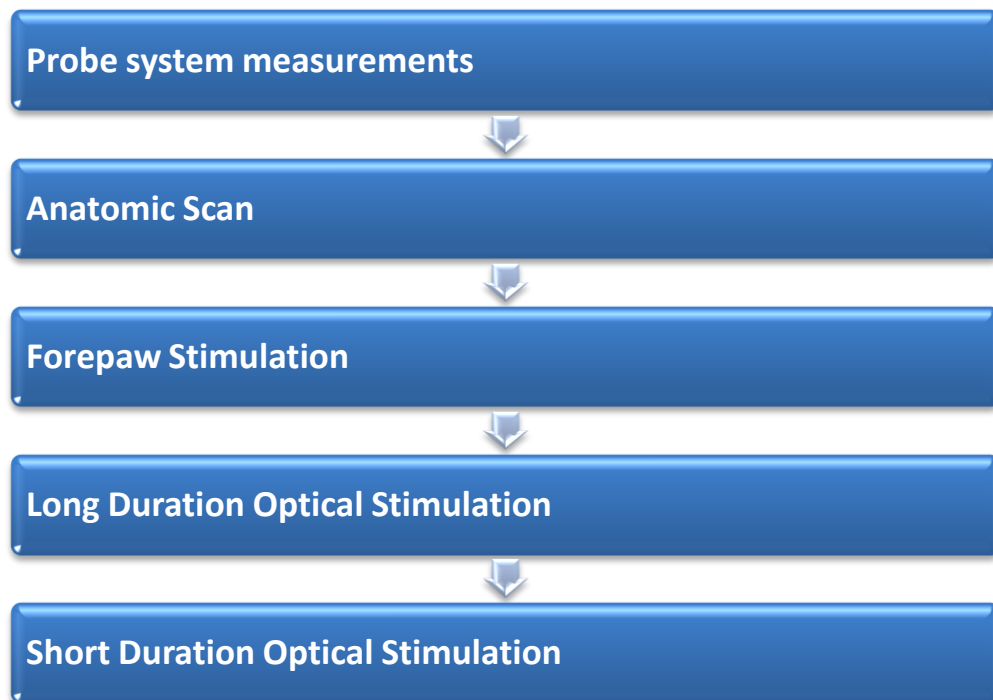
Figure 43: Diagram of MR scanning protocol used for optogenetic stimulation

Before the MR scanning sequence even began a strict route of preparations were made. First, all procedures described were approved and conducted under the Medical College of Wisconsin Institutional Animal Care and Use Committee. The animal was first anesthetized and brought

into the scanner room. Inside the scanner room the animal was mounted to the MR gurney with a customized head mount where the optical fiber could connect to the probe. Once the animal was mounted and all vital signs had stabilized the optical fiber was connected to the probe. To ensure the optical fiber was properly connected and the light was being delivered into the probe, a fiber optic probe system was used. The fiber optic probe system was developed as part of another project to excite and measure the fluorescence at the end of a fiber optic probe [40]. Because ChR2 is tagged with a fluorescent protein, the probe system can determine the presence of ChR2 before beginning the MR scans. Confirmation of the ChR2 fluorescent protein tag confirms that the optical stimulation is reaching the ChR2 and helps to rule out uncertainty in the optical stimulation system. Once the fluorescent signal has been confirmed the animal is placed in the bore of the MR scanner and the imaging sequence begins.

At the beginning of the scanning sequence a series of images are collected in order to set the scan parameters. The first set of scans in the sequence are the anatomical scans that provide the three dimensional geography in order to set up an ROI. A dorsal slice of the brain can be seen in Figure 44 where a 15 slice array has been assigned for functional scanning. Using the anatomical scans provides a reference point so that scan can be compared and repeated in the future.
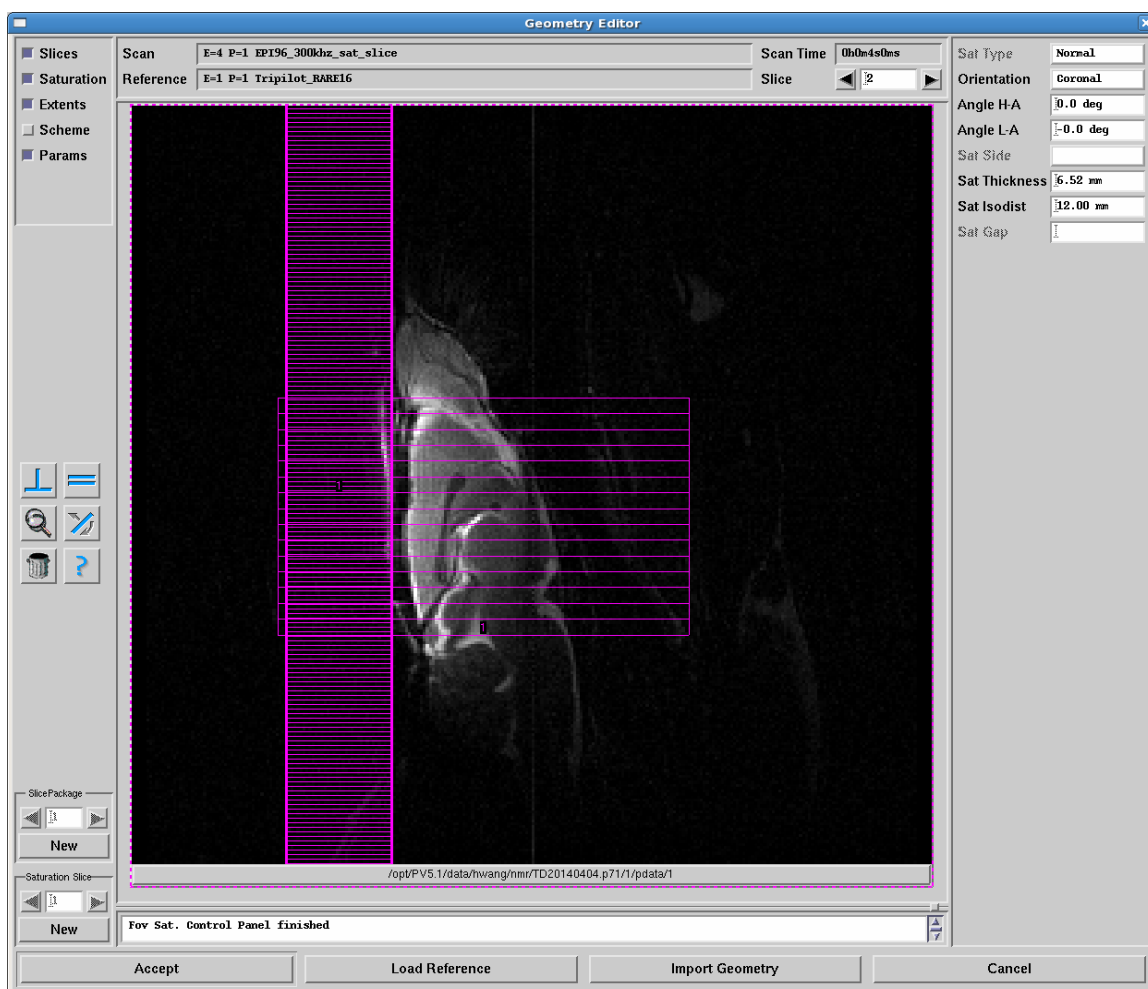
Figure 44: Screen shot of MR user interface of functional slice orientation based on anatomic scan.

After the functional ROI is established the stimulation sequence of the scanning protocol begins

as in Figure 43. To quantify the BOLD signal that is recorded electrical stimulation is applied

during the same scanning session as the Optical stimulation. Electrical stimulation is kept

constant at 1 mA, 15Hz with a 2 second duration, which is applied to the forepaw. The

stimulation produces a BOLD signal in the sensory cortex during each scan and can be used as a

metric for comparison with Optogenetic stimulation. Following the electric stimulation, optical

stimulation is applied through the fiber optic probe and pulsed for a 2-20 second duration at

15Hz. The amplitude of the optical power launched into the fiber can be increased or decreased based on the amount of stimulation required. Each optical and electric stimulation scan is repeated 3 or more times in order to average signals and reduce background noise. These established scanning protocols are repeated for each MR scanning session and from animal to animal. Following the protocol both reduces the sources of error and allows for side by side data comparison.

4.4 Results

Preliminary results from the Optogenetic fMRI study have been collected over a 6 month period. Over that time the MR scanning protocol was being continuously revised using a trial and error process. The results obtained and presented here are the product of the final scan protocol previously explained. Preliminary data suggests that the Optogenetic stimulation is producing all of the indicators of a BOLD signal response. Before assuming that the optical stimulation is driving neural activity to produce a BOLD response all of the indicators must be examined.
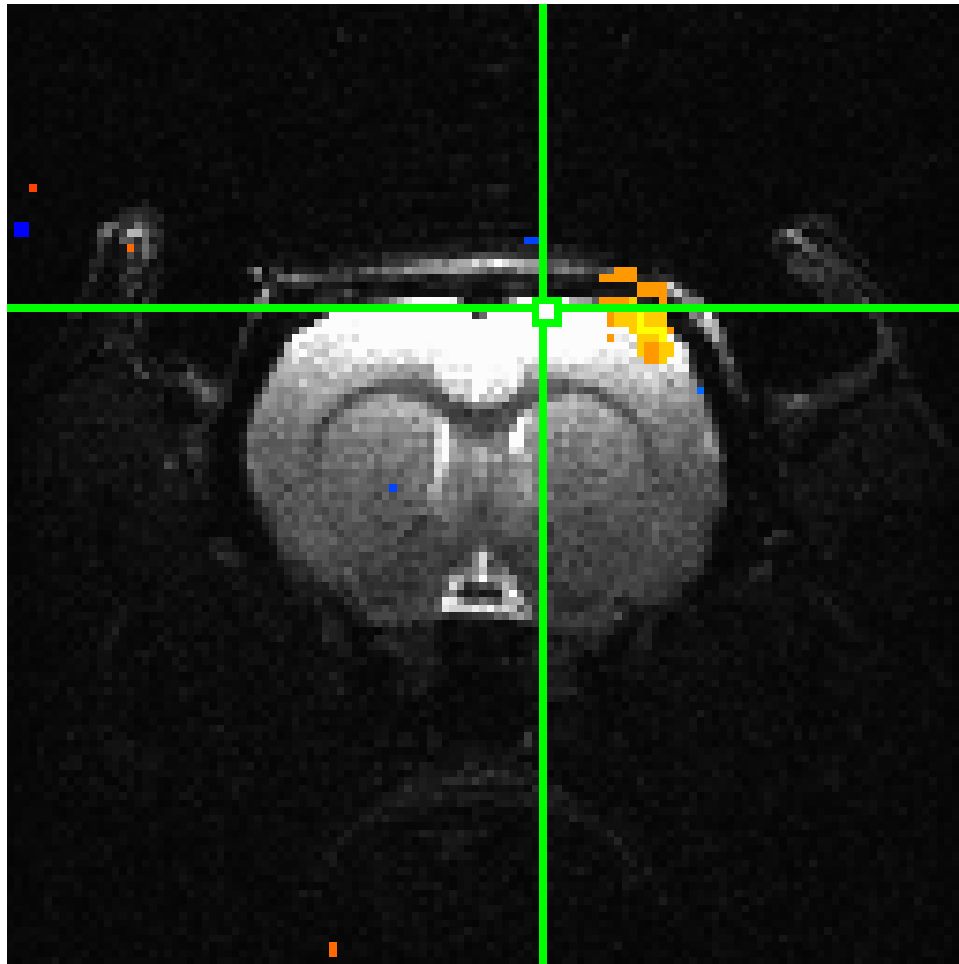
Figure 45: Cross sectional image of brain with BOLD signal following forepaw stimulation, intensity and correlation indicated by color scale

The first stimulation scans used a basic forepaw electric stimulus to produce neural activity in the sensory cortex. Using electric stimulus to create neural activity in the sensory cortex is used as a standard method to establish a functional activity metric [41] [42]. Since the MR scanner and electrical stimulator are synchronized, the BOLD response can be correlated with the applied stimulation over time. Each three dimensional voxel inside the functional image is then color coded based on its time correlation factor (R value). This correlation is then represented by a red or blue color code on the functional image in Figure 45. Voxels above the R threshold

are colored based on their correlation (Red) or anti-correlation (Blue). All other voxels that fall

below the threshold are left gray. The BOLD signal produced by the forepaw stimulation

produced colored pattern in the sensory cortex as expected. The boxes in Figure 46 with the

white background indicate they are above the threshold and plot the BOLD signal over time. The

stimulation pattern is also indicated in red to demonstrate the correlation of the BOLD signal

detected. In the results of the forepaw electric stimulation a very standard BOLD signal is

observed and will be used for direct comparison to the Optogenetic stimulation.
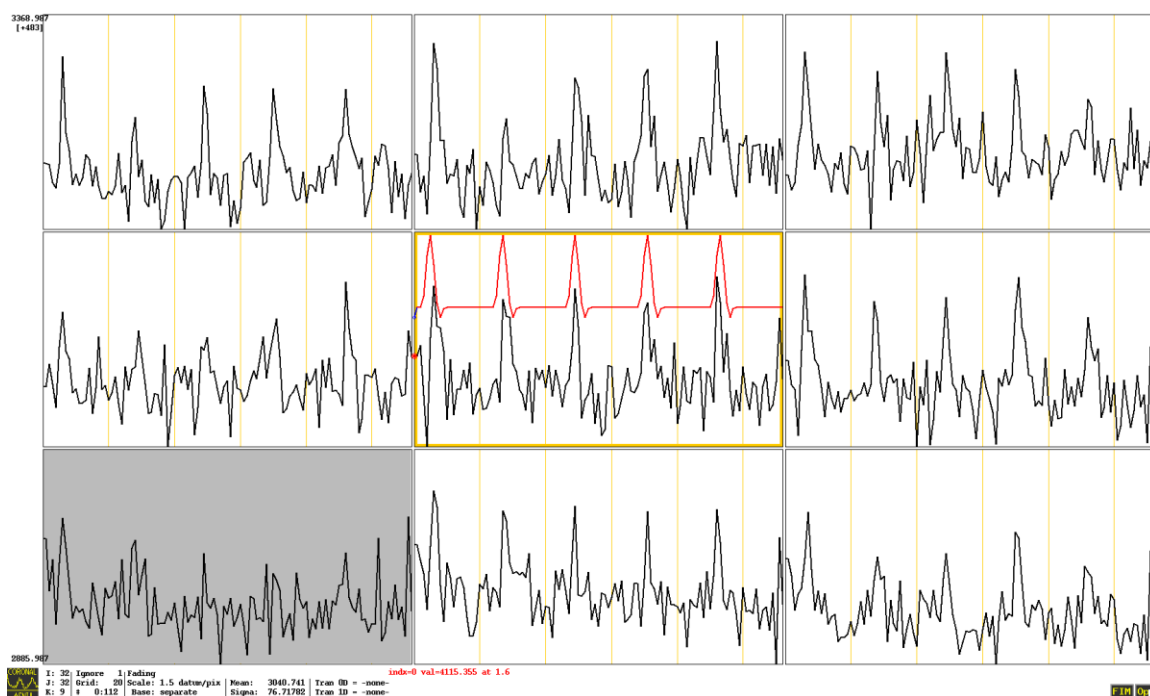
Figure 46: Graphs of BOLD signal over time from selected voxels in cross section image.

The next step in the scanning protocol is to repeat the same stimulation pattern with

Optogenetics. The results of which will also have to be correlated with the stimulation input and

color coded. Again since the optical stimulator is synchronized with the MR scanner the signal

response can be correlated with the applied stimulation. The Optogenetic stimulation was able

to produce a well distinguished BOLD signature in the functional scans which is located near the end of the fiber optic probe. In Figure 47 a strong correlated (Red) and anti-correlated (Blue) BOLD signal is detected near the fiber optic probe. The neighboring Red and Blue signals are not well understood, but the most probable explanation is a large redirection of oxygenated blood [43]. The detected BOLD signal is a strong indicator of Optogenetic stimulation based on the location of the activity.
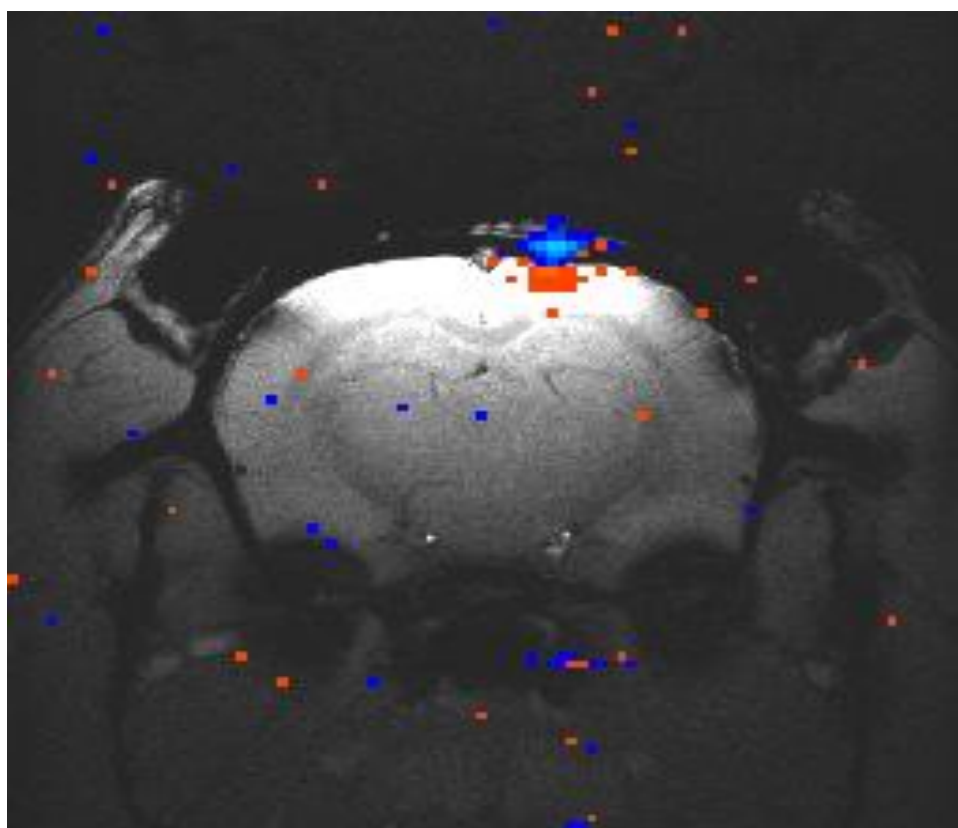
Figure 47: Cross sectional image of brain with BOLD signal following optogenetic stimulation.
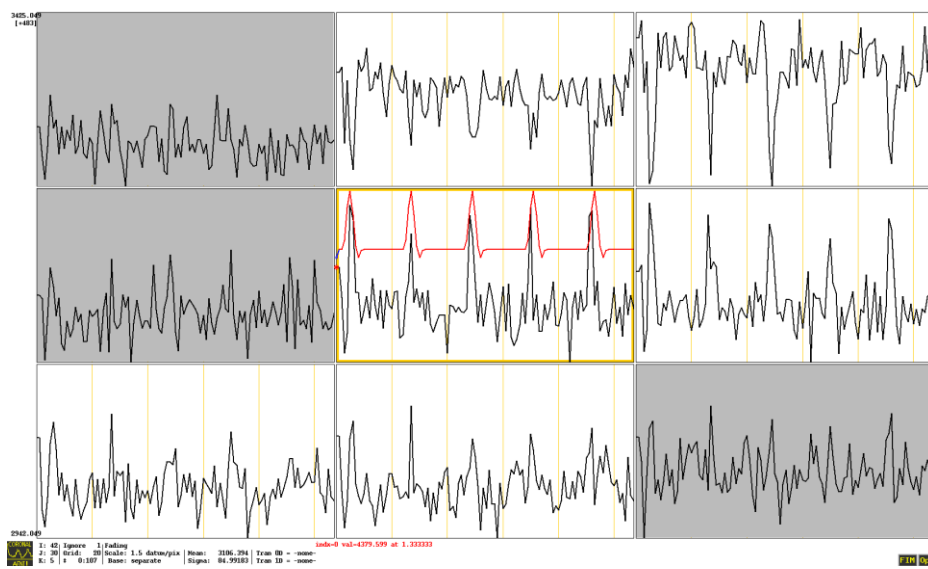
Figure 48: Graphs of BOLD signal over time from selected voxels in cross section image following optogenetic stimulation.

Another method of validating the measure the BOLD signal as a result of Optogenetic stimulation is to vary the stimulation parameters. By increasing or decreasing the stimulation duration along with intensity of stimulation the BOLD signal will vary as well. At first, a relatively long 20 second stimulation duration was used while applying low ($1mW/mm^2$) to high ($5mW/mm^2$) optical stimulation. This was then repeated for 10, 5 and 2 second stimulation durations over the same scanning session. To quantify the results from more than one voxel, all voxels above the set threshold were averaged. The results of this variation of optical stimulation are shown in Figure 49, where the number of averaged voxels is in red. Based on the preliminary collected data the BOLD signal follows the optical stimulation parameters applied. This provides another indicator that the Optogenetic stimulation is producing neural activity indicated by the recorded BOLD signal.
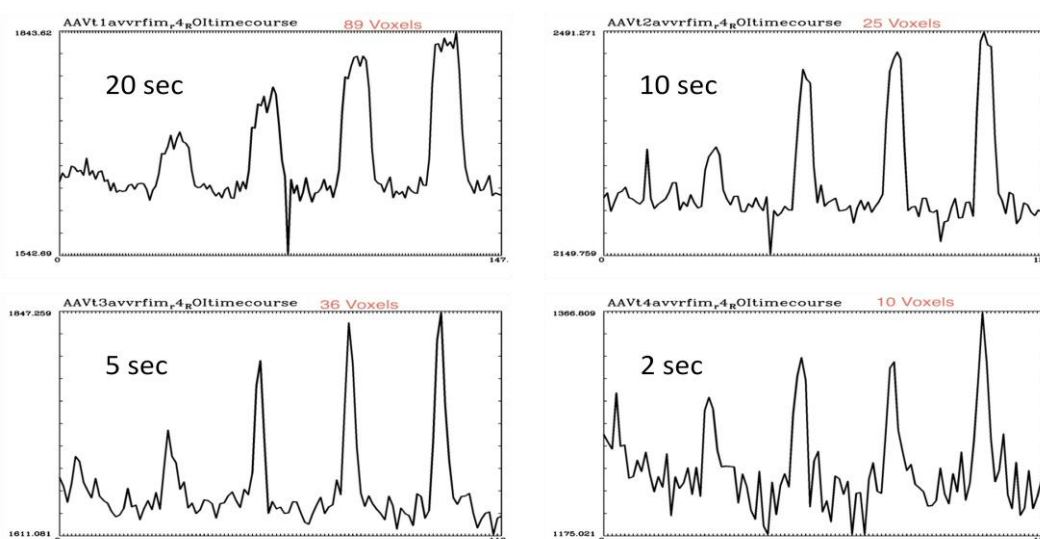
Figure 49: Graphs of BOLD signal following optogenetic stimulation as the duration and optical power was increase.

Finally, in order to directly compare the forepaw stimulation with the optical stimulation, the

Hemodynamic Response Function (HRF) was calculated. To calculate the HRF of both the

electrical and optical stimulation the BOLD data from all voxels above the threshold in Figure 51

and Figure 53 had to be averaged. All 5 stimulations within the scan also had to be averaged

together as well. The result of averaging all of the data is the HRF, characterized by a rapid

increase in signal, followed by an undershoot and dampened oscillation pattern. In the electrical

stimulation all of the HRF characteristics are present in the data collected. In the optical

stimulation BOLD signal all of the HRF characteristics are present as well. The only differences

between the two stimulation methods is first the amplitude of the signal and second the

decreased response time of the optical stimulation. This result is another strong indicator of

neural activity indicated by the BOLD signal. But the data also raises questions in regards to the

amplitude and time scale of the Optogenetic HRF which are still being investigated.
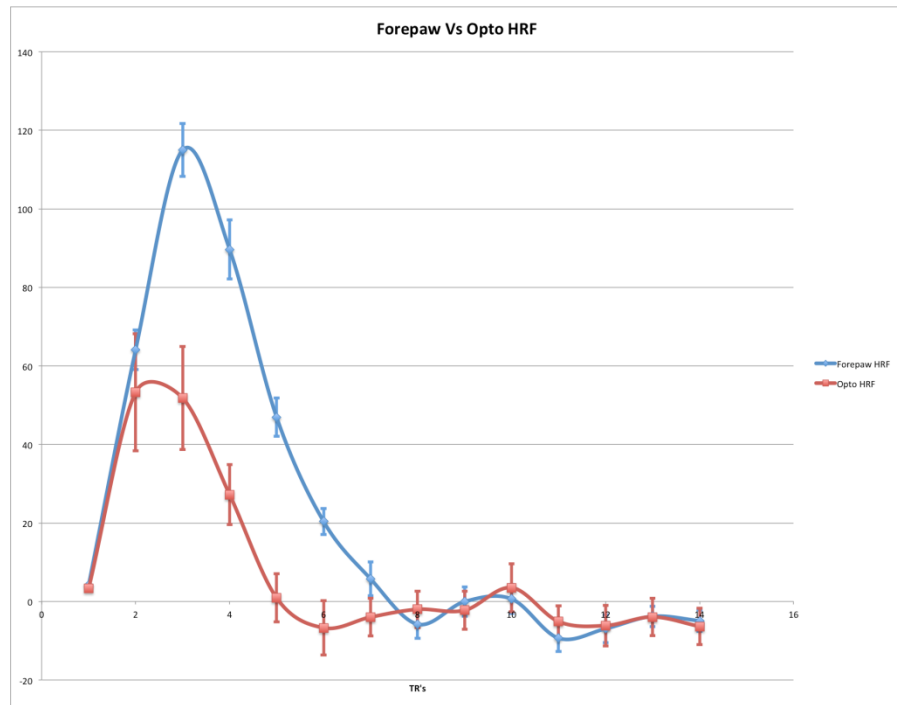
Figure 50: Graph of hemodynamic response function of both the forepaw stimulation (blue) and optogenetic stimulation (red).

4.5 Summary

Combining Optogenetics with functional MR imaging opens up new avenues of research not possible before. This project aimed to establish the necessary tools in order to create new ways in which to study the fundamental functions of the brain. By customizing hardware and developing software, new tools were created to work with the MR scanner. The tools developed may be the first step for future projects that can build on what has been done in this project.

By establishing the protocols needed to validate the data that has been recorded the proof of concept necessary for future experiments has been established. Going forward, more data will be collected using the same protocols with more animals, which will lead to further advancement of the technique. The scanning techniques presented here will then be expanded upon as the project continues to develop and mature.

Because the data from this project is preliminary, more work is still needed to validate the BOLD signal and corresponding neural activity. That said, the indicators presented here all show strong signs of the BOLD signal in response to neural activity. Repeating the experiments established here will help solidify the preliminary results obtained already. Future data generated using the procedures discussed in this chapter will help to solve some of the questions surrounding the functions of the brain.

Chapter 5: Conclusion

As initially stated, monitoring hemodynamics as an indicator of neural activity is a commonly used method in neuroscience. New techniques were developed to study the relationship between hemodynamics and neural coupling. The optical techniques presented in this thesis were pursued in order to provide new tools for neural monitoring and make *in vivo* measurements. The first of the two projects utilized Optogenetics along with OCT technology. Using a system designed and built in the lab the project was successfully able to stimulate neural activity and monitor hemodynamics simultaneously. The second project incorporated fMRI technology and its ability to image the BOLD signal, an indicator of neural activity. Using Optogenetics, the BOLD signal was detected in the same location as the expected neural activity.

In the first project the brain was first stimulated and the resulting hemodynamics were recorded. The neural stimulation was produced optically using a new technology known as Optogenetics. To record the resulting hemodynamics an OCT system was used to monitor blood velocity and flow. The two optical techniques were used side by side without any interference due to the fact that one operates in the visible range while the other operates in the infrared spectrum. The hardware and software were all developed and created in the lab so that the system could perform its required tasks.

Additionally, the second project used Optogenetics as well in order to stimulate neural activity and monitor the resulting hemodynamics. For this project instead of an optical monitoring

system a MR scanner was used to monitor the entire brain. Again hardware and software was developed so that the optical and MR systems functioned simultaneously.

5.1 Optogenetic OCT

The primary goal of the Optogenetic OCT project was to simultaneously stimulate neural activity and image the resulting hemodynamics. In order to achieve this goal three primary steps were taken. First an OCT system was designed and built in the lab capable of both stimulating the brain and measuring *in vivo* hemodynamics. Second the necessary software and image processing tools were developed to both run and process the data recorded by the OCT system. And third, an experimental approach was planned in order to stimulate the brain and record its hemodynamics simultaneously.

Following the experiment, the data was monitored and recorded for post processing. The primary indicators that were observed satisfied all of the proposed results. Primarily, the data allowed identification of hemodynamic changes such as dilation in blood vessels and capillaries with Optogenetic stimulation. In addition, changes were also seen in blood flow and velocity with stimulation. Also, the changes in blood flow and velocity were quantified and plotted over time to demonstrate the coupling between the neural activity and the hemodynamic response. Finally, the procedure was repeated with control animals with no signs of significant changes in any of the same indicators.

5.2 Optogenetic fMRI

The Optogenetic fMRI project's primary goal was to establish a proof of concept. The objective was to combine optical technology and MR technology so that neural activity could be precisely stimulated. To achieve this goal first a methodology was developed in order to stimulate optically sensitive neurons inside an MR scanner. Second scans were performed and data was collected to gather evidence of neural activity and demonstrate the BOLD indicator. And finally, using the data collected, a hemodynamic response function was calculated for the Optogenetic stimulation. In the results presented the BOLD signal was correlated with delivered optical stimulation, similar to previously reported results [37]. The BOLD signal also followed the modulated optical stimulation in duration and amplitude. Finally the hemodynamic response function was found and compared using electric forepaw and Optogenetic stimulation. In the end the concept of stimulating neural activity within a MR scanner using Optogenetics was validated and will provide a very robust tool for future studies.

5.3 Future work

As a result of the successful proof of concept of the Optogenetic OCT system many new projects and studies are now possible. The first goal of any new project would be optimization of the current hardware. Improving the lens system opens up new imaging possibilities deeper in the brain with higher resolutions. An ideal lens system would be capable of imaging capillary networks over 1 mm inside the cortex. In addition a more sensitive detector, line CCD camera, would decrease background noise and improve the SNR. A stronger signal would also improve resolution, but could also make the velocity and flow measurements more accurate as well.

Aside from hardware improvements, new studies are now also possible with the OCT system. Using the experience and knowledge gained from the initial study, additional studies in neural pathologies are now possible. Cerebral vasculature effects of major disease models such as: stroke, Alzheimer's, diabetes and others, can now be studied *in vivo*. The additional capability of Optogenetic stimulation of neural activity will also provide new possibilities when investigating neural vasculature coupling in disease models. Using the new Optogenetic OCT system as a new tool in neuroscience offers new possibilities not available before.

Building off of the proof of concept presented by combining Optogenetics and functional imaging using MR technology, many new studies and possibilities are now open. One which will be pursued in the nearby future will be stimulating specific patterns of neural activity in the MR scanner. The goal of which will be to produce predefined neural network activity by applying an array of optical stimulation to the surface of the cortex while in the MR scanner. The goal of which will be to stimulate the retinas and monitor the resulting functional image. Following this, optical stimulation will be applied in patterns to the visual cortex in order to produce similar functional images. Using the initial proof of concept, Optogenetically stimulating or even controlling the brain inside the a fMRI is now a reality, opening many new possibilities.

Bibliography

[1] S. S. V. S. M. Y. K. N. P. S. P. T. A. D. S. V. M. F. a. D. B. Anna Devor, "Frontiers in optical imaging of cerebral blood flow," *Journal of Cerebral Blood Flow and Metabolism,* vol. 32, pp. 1259-1276, 2012.

[2] E. S. Boyden, F. Zhang, E. Bamberg, G. Nagel and K. Deisseroth, "Millisecond-timescale, genetically targeted optical control of neural activity," *Nature neuroscience,* vol. 8, no. 9, pp. 1263-1268, 2005.

[3] L. Fenno, O. Yizhar and K. Deisseroth, "The development and application of optogenetics," *Annual review of neuroscience,* vol. 34, pp. 389-412, 2011.

[4] V. J. Srinivasan, J. Y. Jiang, M. A. Yaseen, H. Radhakrishnan, W. Wu, S. Barry, A. E. Cable and D. A. Boas, "Rapid volumetric angiography of cortical microvasculature with optical coherence tomography," *Optics letters,* vol. 35, no. 1, pp. 43-45, 2010.

[5] J. G. Fujimoto, "Optical coherence tomography for ultrahigh resolution in vivo imaging," *Nature Biotechnology,* vol. 21, no. 11, 2003.

[6]   V. J. Srinivasan, H. Radhakrishnan, J. Y. Jiang, S. Barry and A. E. Cable, "Optical coherence microscopy for deep tissue imaging of the cerebral cortex with intrinsic contrast," *Optics express,* vol. 20, no. 3, pp. 2220-2239, 2012.

[7]   S. L. J. Z. M. S. H. S. R. H. A. G. Ruikang K. Wang, "Three dimensional optical angiography," *Optics Express,* vol. 15, no. 7, 2007.

[8]   W. D. C. K. H. a. T. L. A F Fercher, "OCT Principals and Applications," *Reports on the progress of physics,* vol. 66, p. 239–303, 2003.

[9]   D. J. K. W. R. W. a. K. A. P. Andrei B. Vakhtin, "Common-path interferometer for frequency-domain," *Applied Optics,* vol. 42, no. 34, 2003.

[10] S. H. Yun, G. J. Tearney, B. E. Bouma, B. H. Park and J. F. de Boer, "High-speed spectral-domain optical coherence tomography at 1.3 μm wavelength," *Optics express,* vol. 11, no. 26, p. 3598–3604, 2003.

[11] K. Deisseroth, "Optogenetics," *Nature methods,* vol. 8, no. 1, pp. 26-29, 2010.

[12] B. V. Zemelman, G. A. Lee, M. Ng and G. Miesenböck, "Selective Photostimulation of

Genetically ChARGed Neurons," *Neuron,* vol. 33, no. 1, pp. 15-22, 2002.

[13] R. Pashaie, P. Anikeeva, J. H. Lee, R. Prakash, O. Yizhar, M. Prigge, D. Chander, T. Richner and J. Williams, "Optogenetic Brain Interfaces," *IEEE reviews in biomedical engineering,* pp. 1-1, 2013.

[14] K. Preuschoff, "Physiological Basis of the BOLD Signal," in *University of Zurich*, 2008.

[15] J. Y. Lin, M. Z. Lin, P. Steinbach and R. Y. Tsien, "Characterization of Engineered Channelrhodopsin Variants with Improved Properties and Kinetics," *Biophysical Journal,* vol. 96, no. 5, pp. 1803-1814, 2009.

[16] J. Culham, "Introduction to Funcational MRI," in *Western University*, London, Canada, 2013.

[17] T. M. L. A. R. K. a. D. W. T. S Ogawa, "Brain magnetic resonance imaging with contrast dependent on blood oxygenation," *Proc. Nati. Acad. Sci. USA ,* vol. 87, no. 24, 1990.

[18] S. B. Owen J. Arthurs, "How well do we understand the neural origins of the fMRI BOLD signal?," *Trends in NeuroSciences,* vol. 25, no. 1, 2002.

[19] A. C. H. W. S. G. a. D. G. A. David J. Heeger, "Spikes versus BOLD: what does neuroimaging

tell us about neuronal activity?," *Nature Neuroscience,* vol. 3, no. 7, 2000.

[20] S. J. M. &. B. A. MacVicar, "Calcium transients in astrocyte endfeet cause cerebrovascular constrictions," *Nature,* vol. 431, pp. 195-199, 2004.

[21] Y. B. S. a. A. Das, "Anticipatory hemodynamic signals in sensory cortex not predicted by local neuronal activity," *Nature,* vol. 457, 2009.

[22] C. R. F. a. P. W. Stroman, "The role(s) of astrocytes and astrocyte activity in neurometabolism, neurovascular coupling, and the production of functional neuroimaging signals," *European Journal of Neuroscience,* vol. 33, no. 4, 2011.

[23] G. e. al., "Brain metabolism dictates the polarity of astrocyte control over arterioles," *Nature,* vol. 456, pp. 745-749, 2008.

[24] D. &. V. Duvernoy, "Cortical blood vessels of the human brain," *Brain Research Bulletin,* vol. 7, no. 5, 1981.

[25] H. e. al, "Blood Capillary Distribution Correlates with Hemodynamic-based Functional Imaging in Cerebral Cortex," *Cerebral Cortex,* vol. 12, no. 3, 2002.

[26] F. Zhang, L.-P. Wang, M. Brauner, J. F. Liewald, K. Kay, N. Watzke, P. G. Wood, E. Bamberg, G. Nagel, A. Gottschalk and K. Deisseroth, "Multimodal fast optical interrogation of neural circuitry," *Nature,* vol. 446, no. 7136, pp. 633-639, 2007.

[27] R. P. Aylward, "Advances and technologies of galvanometer-based optical scanners," in *SPIE Proceedings*, 1999.

[28] L. Dickson, "High dispersion diffraction grating including multiple holographic optical elements". USA Patent US 7321466 B2, 22 January 2008.

[29] J. Lee, W. Wu, J. Y. Jiang, B. Zhu and D. A. Boas, "Dynamic light scattering optical coherence tomography," *Optics Express,* vol. 20, no. 20, pp. 22262-22277, 2012.

[30] T. Bajraszewski, M. Wojtkowski, M. Szkulmowski, A. Szkulmowska, R. Huber and A. Kowalczyk, "Improved spectral optical coherence tomography using optical frequency comb," *Optics Express,* vol. 16, no. 6, pp. 4163-4176, 2008.

[31] M. Szkulmowski, A. Szkulmowska, T. Bajraszewski, A. Kowalczyk and M. Wojtkowski, "Flow velocity estimation using joint Spectral and Time domain Optical Coherence Tomography," *Optics Express,* vol. 35, no. 1, pp. 6008-6025, 2008.

[32] S. F. e. a. Farid Atry, "Hemodynamic Response of Cortical Tissue to Optogenetic Stimulation in Transgenic Mice," *IEEE Transactions on Biomedical Engineering,* Submitted Feburary 2014.

[33] Z. Zhi, W. Cepurna, E. Johnson, T. Shen, J. Morrison and R. K. Wang, "Volumetric and quantitative imaging of retinal blood flow in rats with optical microangiography," *Biomedical Optics Express,* vol. 2, no. 3, pp. 579-591, 2011.

[34] P. J. Drew, A. Y. Shih, J. D. Driscoll, P. M. Knutsen, P. Blinder, D. Davalos, K. Akassoglou, P. S. Tsai and D. Kleinfeld, "Chronic optical access through a polished and reinforced thinned skull," *Nature Methods,* vol. 7, no. 12, pp. 981-984, 2010.

[35] J. I. Szu, . M. M. Eberle, C. L. Reynolds, M. S. Hsu, Y. Wang, C. M. Oh , M. S. Islam, B. H. Park and D. K. Binder, "Thinned-skull Cortical Window Technique for In Vivo Optical Coherence Tomography Imaging," *Journal of visualized experiments,* vol. 69, p. e50053, 2012.

[36] I. K. U. K. J. B. H. A. A. Y. N. K. R. L. B. A. M. G. I. M. a. E. S. B. M. Desai, "Mapping brain networks in awake mice using combined optical neural control,," *Journal of Neurophysiol,* vol. 105, p. 1393–1405, 2010.

[37] R. D. V. G. F. Z. I. G. D.-S. K. L. E. F. Jin Hyung Lee, "Global and local fMRI signals driven by

neurons defined optogenetically by type and wiring," *Nature,* vol. 465, pp. 788-792, 2010.

[38] M. D. U. K. J. B. M. H. A. M. G. E. S. B. R. L. B. a. C. I. M. Itamar Kahn, "Characterization of the Functional MRI Response Temporal Linearity via Optical Control of Neocortical Pyramidal Neurons," *Journal of Neuroscience,* vol. 31, no. 42, 2011.

[39] R. P. a. R. Falk, "Spectral analysis of whisking output via optogenetic modulation of vibrissa cortex in rat," *Biomedical Optics Express,* vol. 4, no. 1, 2013.

[40] R. P. a. R. Falk, "Single Optical Fiber Probe for Fluorescence Detection and Optogenetic Stimulation," *IEEE: Biomedical Engineering,* vol. 60, no. 2, 2013.

[41] e. a. Artem G. Goloshevskya, "BOLD fMRI and somatosensory evoked potentials are well," *Brain Researcher,* vol. 1195, pp. 67-76, 2008.

[42] O. G. a. M. P. Joanna K. Huttunen, "Coupling between simultaneously recorded BOLD response and," *NeuroImage,* vol. 39, pp. 775-785, 2008.

[43] M. A. A. O. &. N. K. L. Amir Shmuel, "Negative functional MRI response correlates with decreases in neuronal activity in monkey visual area V1," *Nature Neuroscience,* vol. 9, pp. 569 - 577, 2006.

[44] Z. Yaqoob, J. Wu, E. J. McDowell, X. Heng and C. Yang, "Methods and application areas of endoscopic optical coherence tomography," *Journal of biomedical optics,* vol. 11, no. 6, p. 063001, 2006.

[45] H.-T. Xu, F. Pan, G. Yang and W.-B. Gan, "Choice of cranial window type for in vivo imaging affects dendritic spine turnover in the cortex," *Nature Neuroscience,* vol. 10, no. 5, pp. 549-551, 2007.

[46] Y. Wang and R. K. Wang, "Autocorrelation optical coherence tomography for mapping transverse particle-flow velocity," *Optics Letters,* vol. 35, no. 21, pp. 3538-3540, 2010.

[47] H. Wang, J. Zhu and T. Akkin, "Serial optical coherence scanner for large-scale brain imaging at microscopic resolution," *NeuroImage,* vol. 84, p. 1007–1017, 2014.

[48] S. Meissner, L. Knels , A. Krueger , T. Koch and E. Koch, "Simultaneous three-dimensional optical coherence tomography and intravital microscopy for imaging subpleural pulmonary alveoli in isolated rabbit lungs," *Journal of biomedical optics,* vol. 14, no. 5, p. 054020, 2009.

[49] I. N. Christie, J. A. Wells, P. Southern, N. Marina, S. Kasparov, A. V. Gourine and M. F. Lythgoe, "fMRI response to blue light delivery in the naïve brain: Implications for combined optogenetic fMRI studies," *NeuroImage,* vol. 66, p. 634–641, 2013.

[50] R. K. W. a. L. An, "Doppler optical micro-angiography for volumetric imaging of vasculature perfusion in vivo," *Optics Express,* vol. 17, no. 11, 2009.

[51] A. M. Davis, F. G. Rothenberg, J. A. Izatt and N. Shepherd, "In vivo spectral domain optical coherence tomography volumetric imaging and spectral Doppler velocimetry of early stage embryonic chicken heart development," *Journal of the Optical Society of America A,* pp. 3134-3143, 2008.

[52] S. Meissner, L. Knels , A. Krueger , T. Koch and E. Koch, "Simultaneous three-dimensional optical coherence tomography and intravital microscopy for imaging subpleural pulmonary alveoli in isolated rabbit lungs," *Journal of Biomedical Optics,* vol. 14, no. 5, p. 054020, 2009.